Neuron
Article

BAD-Dependent Regulation of Fuel Metabolism and K_{ATP} Channel Activity Confers Resistance to Epileptic Seizures

Alfredo Giménez-Cassina,[1,2] Juan Ramón Martínez-François,[3] Jill K. Fisher,[1] Benjamin Szlyk,[1] Klaudia Polak,[1] Jessica Wiwczar,[1] Geoffrey R. Tanner,[3] Andrew Lutas,[3] Gary Yellen,[3,*] and Nika N. Danial[1,2,*]
[1]Department of Cancer Biology, Dana-Farber Cancer Institute, Boston, MA 02215, USA
[2]Department of Cell Biology
[3]Department of Neurobiology
Harvard Medical School, Boston, MA 02115, USA
*Correspondence: gary_yellen@hms.harvard.edu (G.Y.), nika_danial@dfci.harvard.edu (N.N.D.)
DOI 10.1016/j.neuron.2012.03.032

SUMMARY

Neuronal excitation can be substantially modulated by alterations in metabolism, as evident from the anticonvulsant effect of diets that reduce glucose utilization and promote ketone body metabolism. We provide genetic evidence that BAD, a protein with dual functions in apoptosis and glucose metabolism, imparts reciprocal effects on metabolism of glucose and ketone bodies in brain cells. These effects involve phosphoregulation of BAD and are independent of its apoptotic function. BAD modifications that reduce glucose metabolism produce a marked increase in the activity of metabolically sensitive K_{ATP} channels in neurons, as well as resistance to behavioral and electrographic seizures in vivo. Seizure resistance is reversed by genetic ablation of the K_{ATP} channel, implicating the BAD-K_{ATP} axis in metabolic control of neuronal excitation and seizure responses.

INTRODUCTION

Neuronal electrical activity is tightly integrated with mitochondrial nutrient and energy metabolism in the brain. In addition to buffering intracellular calcium and generating ATP for proper maintenance of ion homeostasis, mitochondria can influence neuronal function by changing redox balance and availability of intermediary metabolites for biosynthetic processes (MacAskill et al., 2010; Nicholls, 2009). Although glucose is the predominant mitochondrial fuel utilized by the brain, neural cells can metabolize alternative carbon substrates, such as ketone bodies, under conditions of glucose limitation or dietary restrictions (Zielke et al., 2009). The capacity of mitochondria to process alternate energy substrates, such as carbohydrates and ketone bodies, may influence neuronal excitability. For example, the ketogenic diet (KD), which reduces glucose metabolism and promotes the breakdown of fatty acids to generate ketone bodies, has shown efficacy in many cases of pharmacoresistant epilepsy (Hartman et al., 2007; Neal et al., 2009; Thiele, 2003).

The potent effect of increased ketone body metabolism on epilepsy in humans points to a link between mitochondrial fuel utilization and neuronal excitability. However, the molecular underpinnings of this link are not fully understood. Numerous mechanisms have been proposed (Schwartzkroin, 1999), including alterations in gene expression (Garriga-Canut et al., 2006) and changes in the levels of metabolic products and byproducts, such as ATP (DeVivo et al., 1978), amino acids (Dahlin et al., 2005; Yudkoff et al., 2001), reactive oxygen species, and glutathione (Jarrett et al., 2008). Moreover, ketone bodies can alter the open probability of the metabolically responsive ATP-sensitive potassium (K_{ATP}) channels (Ma et al., 2007; Schwartzkroin, 1999; Tanner et al., 2011). This can lead to reduced firing of neurons and reduced excitability during seizures. Ketone bodies have also been reported to suppress the vesicular release of glutamate, suggesting a link between metabolism and excitatory synaptic transmission (Juge et al., 2010). Other proposed mechanisms for the anticonvulsant effect of KD include elevation of inhibitory neurotransmitter γ-aminobutyric acid (GABA) levels (Wang et al., 2003; Yudkoff et al., 2001), acidosis-induced changes in acid-sensing ion channel 1a (ASIC1a; Ziemann et al., 2008), and changes in the activity of A_1 purinergic receptors (Masino et al., 2011).

Although these mechanisms have provided valuable insights into metabolic regulation of seizure responses, progress in dissecting the link between metabolism and seizure sensitivity has been difficult because of the complex systemic effects of dietary alterations and the relatively modest effect of KD in rodent models of epilepsy. Identification of cell-intrinsic mechanisms and molecular modulators that can simultaneously attenuate glucose metabolism and enhance ketone body consumption without any dietary manipulation may provide a useful molecular handle on understanding the metabolic control of seizure sensitivity.

BAD (BCL-2-associated Agonist of Cell Death) is a member of the BCL-2 family of cell death/survival proteins (Chipuk et al., 2010; Danial and Korsmeyer, 2004; Youle and Strasser, 2008). Separate from its well-established role in apoptosis, BAD modulates glucose metabolism in multiple cell types, including

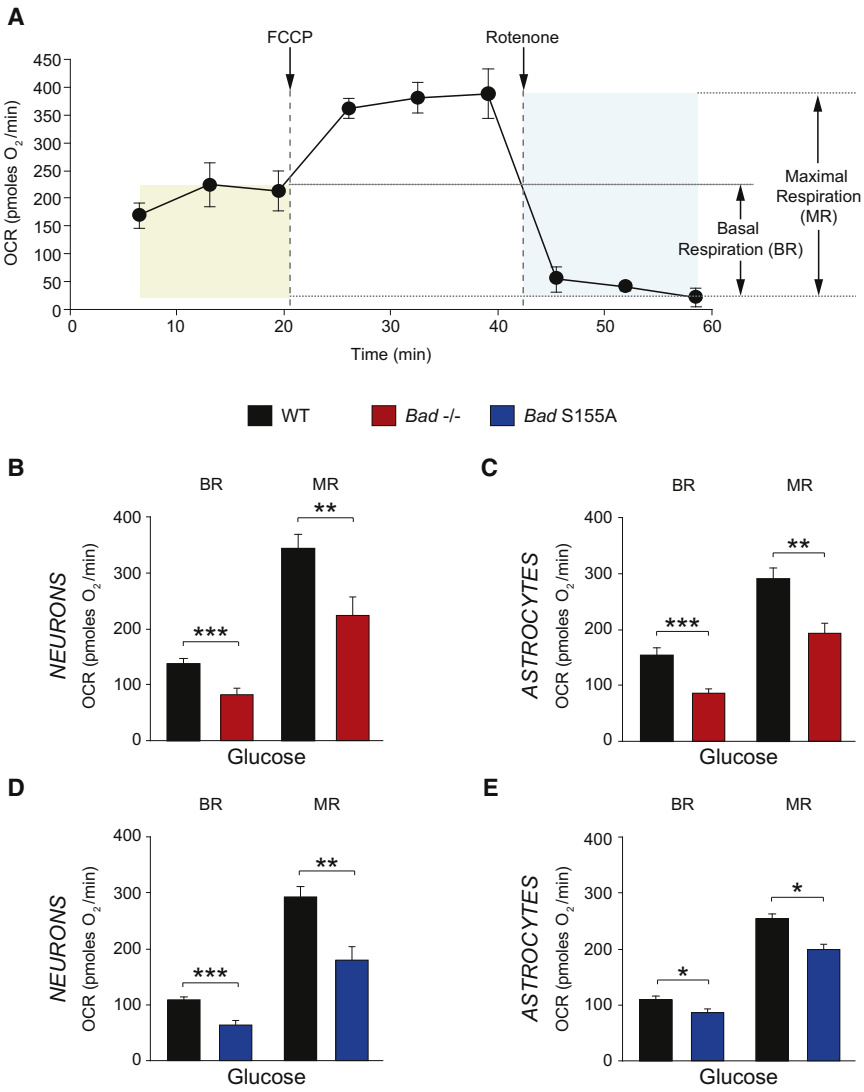

Figure 1. Blunted Mitochondrial Metabolism of Glucose in Primary *Bad*$^{-/-}$ and *Bad*^{S155A} Neurons and Astrocytes

(A) Representative trace of oxygen consumption rate (OCR) measured in real-time indicating basal and maximal respiration rates (BR and MR, respectively).

(B and C) BR and MR in the presence of glucose in primary *Bad*$^{-/-}$ cortical neurons (B) and astrocytes (C).

(D and E) BR and MR in the presence of glucose in primary *Bad*^{S155A} cortical neurons (D) and astrocytes (E). Data in (B) through (E) are presented as mean ± SEM; n = 4–6 independent neuron or astrocyte cultures. *p < 0.05; **p < 0.01; ***p < 0.001; wild-type versus *Bad*$^{-/-}$ or *Bad*^{S155A}; two-tailed Student's t test.

See also Figure S1.

hepatocytes, islet β cells, and fibroblasts (reviewed in Danial, 2008). BAD's dual modalities in apoptosis and metabolism are mediated through a phosphoregulatory mechanism that modifies serine 155 (aa enumeration based on the murine sequence of BAD) located within an alpha helical segment known as the BCL-2 homology (BH)-3 domain (Danial et al., 2008; Datta et al., 2000). In hepatocytes and β cells, serine 155 phosphorylation is required for mitochondrial metabolism of glucose (reviewed in Danial, 2008). In the presence of apoptotic signals, including irreversible cellular damage, dephosphorylated BAD engages the mitochondrial apoptosis machinery through a BH3 domain-dependent mechanism that sensitizes cells to apoptosis.

Reduced glucose metabolism associated with BAD modification is reminiscent of reduced glycolysis and changes in carbon substrate utilization in response to a low carbohydrate diet that promotes ketone body metabolism. This prompted us to investigate potential BAD-dependent changes in seizure responses. Using a combination of genetic models, mitochondrial respirometry, and electrophysiology, as well as electrographic and behavioral studies, we have examined the role of BAD in regulating the preferred carbon substrate utilized by neural cell types and its relevance to neuronal excitability and seizure sensitivity.

RESULTS

Blunted Mitochondrial Metabolism of Glucose in Primary *Bad*$^{-/-}$ and *Bad*^{S155A} Neurons and Astrocytes

Our previous findings—that BAD is required for mitochondrial utilization of glucose in hepatocytes and islet β cells (Danial et al., 2003, 2008)—prompted us to examine how BAD modification may affect glucose metabolism in the brain, where glucose is the predominant carbon and energy substrate. We assessed mitochondrial metabolism of glucose in primary cultures of cortical neurons and astrocytes (Figure S1 available online) by real-time measurement of mitochondrial oxygen consumption rates (OCR). We focused predominantly on two respiratory parameters; glucose-associated basal (steady-state) and maximal respiratory rates (BR and MR, Figure 1A). Mitochondrial MR is an important indicator of a cell's bioenergetic fitness for accommodating any potential rise in metabolic demand (Brand and Nicholls, 2011; Fern, 2003). MR is defined by the fraction of maximal achievable rate of oxygen consumption that is sensitive to the inhibition of mitochondrial respiratory chain activity. To measure MR, neural cultures were first treated with the proton ionophore FCCP to induce maximal OCR prior to treatment with the mitochondrial respiratory chain inhibitor rotenone, and the difference between respiratory rates in response to FCCP and rotenone was measured (Brand and Nicholls, 2011; Figure 1A). When supplied with glucose, neurons and astrocytes derived from *Bad*$^{-/-}$ mice

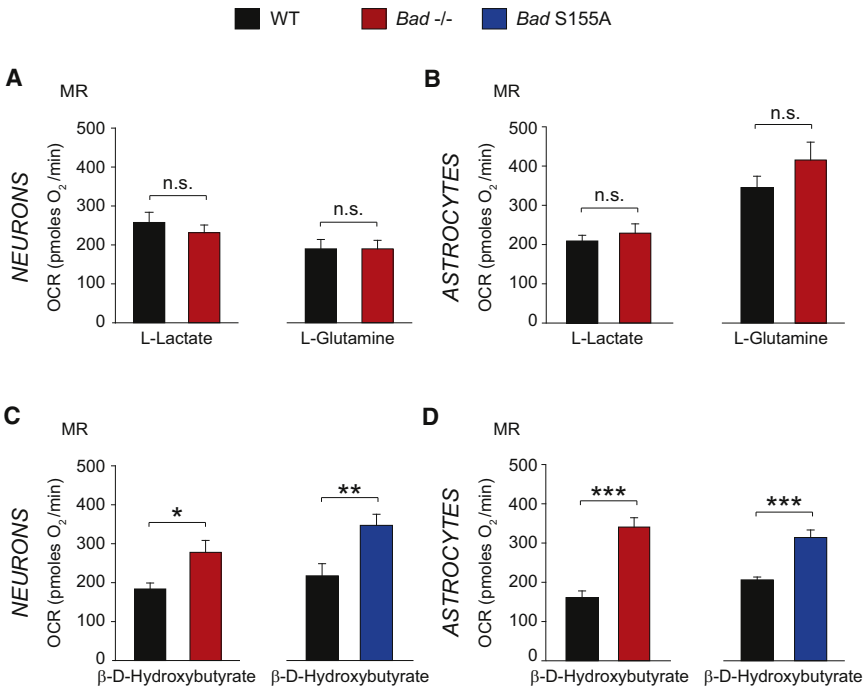

Figure 2. Mitochondrial Metabolism of Non-glucose Fuels in *Bad*$^{-/-}$ and *Bad*^{S155A} Neurons and Astrocytes

(A and B) Mitochondrial maximal respiration (MR) in wild-type and *Bad*$^{-/-}$ neurons (A) and astrocytes (B) supplied with 5 mM L-glutamine or 5 mM L-lactate.

(C and D) MR in the presence of 5 mM β-D-hydroxybutyrate in primary neurons (C) and astrocytes (D) derived from *Bad*$^{-/-}$ and *Bad*^{S155A} mice. Data in (A) through (D) are presented as mean ± SEM; n = 4–6 independent neuron or astrocyte cultures. *p < 0.05; **p < 0.01; ***p < 0.001; n.s. in (A) and (B), nonsignificant; wild-type versus *Bad*$^{-/-}$ or *Bad*^{S155A}; two-tailed Student's t test.

displayed diminished basal OCR and MR compared with wild-type counterparts (Figures 1B and 1C), providing genetic evidence for BAD's relevance in mitochondrial handling of glucose in these cell types.

We have previously shown that phosphorylation of BAD on Ser 155 within its BH3 domain mediates its effect on glucose metabolism (Danial et al., 2008). Consistent with this idea, we found that in primary neurons and astrocytes from mice bearing a non-phosphorylatable knockin allele of BAD (*Bad*^{S155A}), glucose-associated BR and MR were significantly blunted, analogous to *Bad*$^{-/-}$ cells (Figures 1D and 1E). Importantly, as the *Bad* null and S155A alleles have opposite effects on apoptosis (Danial et al., 2008), the comparable diminution of glucose-associated MR in neural cell types derived from both genetic models suggests that modulation of mitochondrial fuel handling stems from metabolic modulation by BAD rather than its effect on apoptosis.

BAD-Dependent Increase in Ketone Body Consumption in the Face of Diminished Glucose Oxidation

Diminished mitochondrial oxidation of glucose warranted investigation whether BAD modification alters consumption of non-glucose fuels in neurons and astrocytes. To test this possibility, we focused on three main physiologic nonglucose carbon substrates that can be utilized by the brain, namely, L-glutamine, L-lactate, and the ketone body β-D-hydroxybutyrate (Zielke et al., 2009). We used mitochondrial MR as an indicator of mitochondrial fuel handling in response to each of these nonglucose fuels.

Bad ablation did not alter mitochondrial handling of carbon substrates, such as L-lactate and L-glutamine, in neurons or astrocytes (Figures 2A and 2B). On the other hand, mitochondrial utilization of β-D-hydroxybutyrate was significantly higher in *Bad*$^{-/-}$ cortical neurons and astrocytes compared with wild-type cells (Figures 2C and 2D), indicating that *Bad* ablation is associated with a selective switch in fuel preference from glucose to ketone body consumption rather than pleiotropic changes in mitochondrial carbon substrate utilization. In addition, a preferential shift to ketone body consumption was observed in cortical neurons and astrocytes derived from *Bad*^{S155A} mice (Figures 2C and 2D), suggesting that BAD phosphorylation on S155 may normally inhibit ketone body utilization. Taken together, these observations are consistent with a BAD-dependent reciprocal programming of mitochondrial glucose versus ketone body consumption that is regulated by the phosphorylation status of its BH3 domain.

Altered Sensitivity of *Bad*$^{-/-}$ and *Bad*^{S155A} Mice to Behavioral Seizures

Metabolic manipulations, such as a high-fat, low-carbohydrate ketogenic diet (KD), can prevent seizures in many cases of pharmacoresistant human epilepsy, as well as in certain rodent models of epilepsy (Stafstrom and Rho, 2004). The reprogramming of carbon substrate metabolism in *Bad*$^{-/-}$ and *Bad*^{S155A} neurons and astrocytes is analogous to ketogenic-diet-induced changes in brain metabolism, namely, reduced glucose metabolism and elevated ketone body consumption. However, these BAD-dependent changes occur in the absence of any dietary manipulations. This led us to hypothesize that metabolic control by BAD may also influence seizure sensitivity in vivo, similar to the KD (Stafstrom and Rho, 2004). To test this hypothesis, we used the chemical proconvulsant kainic acid (KA), which induces acute seizures by stimulating excitatory glutamate receptors (Ben-Ari et al., 1980). Published studies in mice indicate that KD can delay the onset of KA-induced seizures (Jeong et al., 2011; Noh et al., 2003). The seizure responses in BAD mutant and control mice treated with KA were scored using a modified Racine scale as previously described (Ferraro et al., 1997).

Wild-type mice experienced an acute, yet transient, series of seizures that peaked on average between 50–120 min after KA

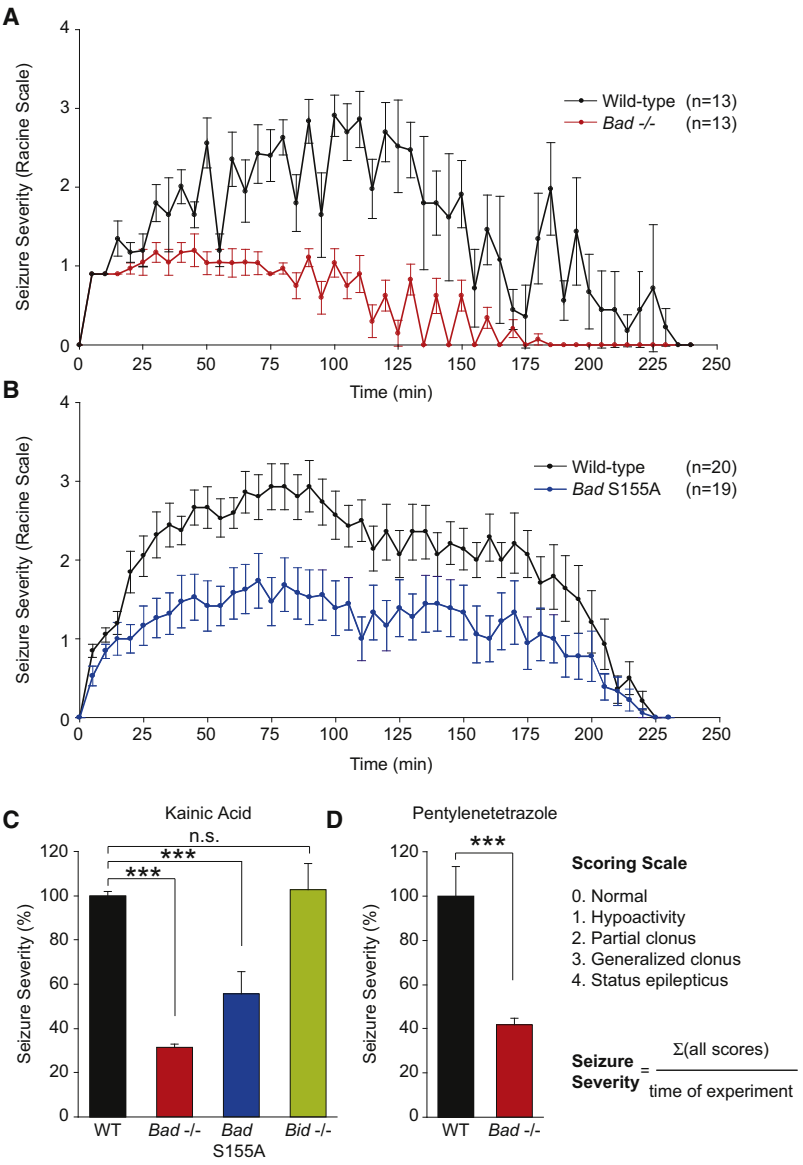

Figure 3. Resistance of *Bad* Genetic Models to Kainic-Acid- and Pentylenetetrazole-Induced Acute Seizures

(A and B) Raw seizure scores in 8- to 10-week-old male $Bad^{-/-}$ (A) and Bad^{S155A} (B) mice compared with wild-type control animals over a 4 hr period after a single i.p. injection of kainic acid (KA) at 30 mg/kg. See also Figure S2.

(C) Integrated seizure severity of the above experimental cohorts and $Bid^{-/-}$ mice similarly treated with KA. The scoring scale and the formula used to derive seizure severity are provided. Wild-type, n = 42; $Bad^{-/-}$, n = 13; Bad^{S155A}, n = 20; $Bid^{-/-}$; n = 9.

(D) Integrated seizure severity in $Bad^{-/-}$ and wild-type mice (n = 16) subjected to a single s.c. injection of pentylenetetrazole (PTZ) at 80 mg/kg monitored over a 70 min period. Data in (A) through (D) are presented as mean ± SEM. ***p < 0.001; n.s., nonsignificant; two-tailed Student's t test.

See also Figures S3, S4, and S5.

administration and then slowly decayed (Figures 3A and 3B). The seizure diaries for individual mice are shown in Figure S2. The majority of wild-type mice (>80%) underwent status epilepticus with very severe tonic-clonic seizures. In striking contrast, $Bad^{-/-}$ mice did not progress in severity to the extent of wild-type animals and were significantly protected from status epilepticus (Figure 3A). Bad^{S155A} mice were similarly resistant to behavioral seizures in this experimental model (Figure 3B). In addition to raw seizure scores based on the modified Racine scale, we integrated individual scores per mouse over the duration of the experiment to better account for seizure severity in mice that died during the experiment (Figure 3C). Seizure severity was significantly diminished in both *Bad* null and S155A knockin mice (Figure 3C). Moreover, seizure resistance in the absence of BAD is not limited to the kainate model. *Bad* null mice were also protected against status epilepticus triggered by pentylenetetrazole (PTZ), which antagonizes GABAergic inhibitory receptors (Bough and Eagles, 1999; Ferraro et al., 1999; Figure 3D).

To determine whether seizure resistance in $Bad^{-/-}$ and Bad^{S155A} mice is accompanied by neurobehavioral abnormalities, we conducted a detailed battery of cognitive and motor function tests. These studies did not reveal any significant differences in *Bad* genetic models compared with control mice (Figure S3). It therefore appears unlikely that these models produce major circuit-level effects that impair normal brain function and might also disrupt seizure mechanisms.

As the *Bad* null and S155A alleles have opposite effects on BAD's apoptotic function (Danial, 2008), the comparable resistance to seizures observed in *Bad* null and S155A mice cannot be explained by changes in apoptosis. To further test for the specificity and selectivity of BAD in this paradigm, BID-deficient mice were examined. BID (BH3-Interacting domain Death agonist) is another BH3-only proapoptotic member of the BCL-2 family similar to BAD but does not affect glucose metabolism (Danial, 2008). *Bid* null mice displayed comparable sensitivity to seizures as was seen in wild-type littermates (Figure 3C). In addition, targeted deletion of another BH3-only proapoptotic molecule BIM (BCL2-Interacting Mediator of cell death) in the brain did not confer resistance against acute seizures (Figure S4). Thus, it appears that the seizure-resistance phenotype of BAD mutant mice is neither related to BAD's apoptotic role nor universally shared among other BCL-2 family members.

Changes in the preferential ability to utilize ketone bodies in the absence of BAD and the attendant resistance to acute seizures may derive from local metabolic alterations in the brain and/or from altered metabolism in the liver, which is the body's main source of ketone body production. Two lines of

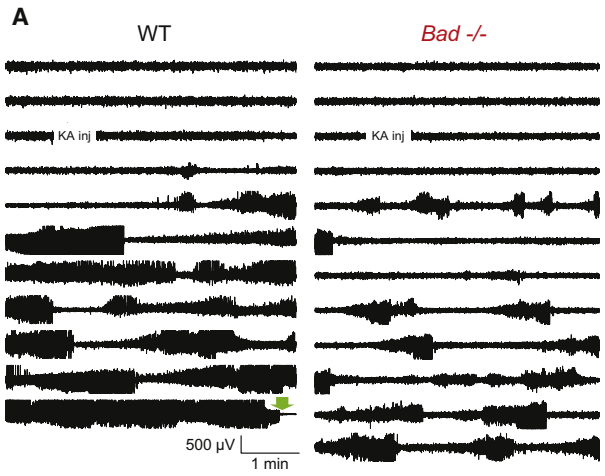

Figure 4. EEGs of Kainic-Acid-Induced Seizure Activity in Wild-Type and *Bad*$^{-/-}$ Animals

(A) A single representative EEG channel recording of approximately 1 hr for each genotype (right frontoparietal electrode). A single i.p. injection of kainic acid (30 mg/kg of body weight) was administered at the indicated time. The green block arrow near the end of the wild-type recording indicates the time of death during generalized tonic-clonic status epilepticus.

(B) The average fraction of time spent in a high-energy spiking period for each genotype during a 30 min period beginning 3 min after injection. EEGs were scored by an investigator blind to the genotype, guided by both the raw EEG traces and a trace of power in the 20–70 Hz band to identify onset and offset of high-energy spiking (typically seen as rapid increases or decreases of $\geq$5 dB in power). Wild-type, n = 17; *Bad*$^{-/-}$, n = 20; mean ± SEM, *p < 0.05 by two-tailed Student's t test. In these cohorts, 9 of 17 wild-type and 0 of 20 *Bad*$^{-/-}$ animals died during status epilepticus.

See also Figure S3.

investigation suggest that seizure protection in the absence of BAD cannot be explained by systemic alterations in ketone body metabolism. First, we have not observed any differences in the serum levels of ketone bodies in these animals (data not shown). Second, liver-specific knockdown of *Bad* does not produce seizure protection in mice (Figure S5), despite fully mimicking the hepatic phenotype of *Bad*$^{-/-}$ mice (data not shown). These results are especially relevant as liver is the chief source of ketone bodies for systemic supply to other tissues. Our observations suggest that local metabolic alterations in the brain of *Bad*$^{-/-}$ animals, rather than systemic changes in ketone body metabolism, most likely contribute to seizure protection in the absence of BAD.

Altered Electrographic Seizures in *Bad*$^{-/-}$ Mice

Seizures produced by kainic acid, as for several other convulsant treatments in rodents, appear first as hypoactivity and focal "limbic seizures" involving automatisms, facial and forelimb clonus, and rearing; these seizures can progress to generalized tonic-clonic seizures and death (Velíšková, 2005). The former are attributed to forebrain or limbic activity, whereas the generalized seizures are thought to be mediated by brainstem or midbrain reticular systems (Browning, 1994). In several rodent seizure models that follow this pattern, clinically useful anticonvulsants, such as phenytoin (Browning et al., 1990), levetiracetam (Klitgaard et al., 1998), and topiramate (Haugvicová et al., 2000), have little effect on the focal seizures but disrupt progression to generalized motor seizures.

A similar protection against generalized seizures in the intraperitoneal (i.p.) kainate model was seen in the behavioral experiments on mice with alteration of BAD. *Bad*$^{-/-}$ mice or *Bad*^{S155A} knockin mice rarely exhibited generalized motor seizures (and when they occurred they were very brief), whereas most control animals had severe generalized seizures, and many control animals died during status epilepticus (Figures 3 and S2).

In addition to noting this marked difference in behavioral seizure response, we performed video-electroencephalographic (EEG) analysis of the behavioral and electrographic seizures in cohorts of wild-type and *Bad*$^{-/-}$ mice subjected to i.p. kainate injection (Figure 4). As expected from the hypothesized deep-brain localization of the generalized motor seizures, the frontal and parietal screw electrodes did not report a clear electrographic correlate to the more severe seizures. They did, however, record high amplitude spiking activity that was usually correlated with the limbic seizures—as the electrographic activity intensified, a typical progression was seen from head movement to rearing with unilateral or bilateral forelimb clonus, which ceased upon the usually sudden cessation of spiking. Overall comparison of electrographic activity was complicated by the death of wild-type animals, often seen ~30 min after KA injection in this cohort; we therefore restricted the analysis to the first 30 min after injection. For the *Bad*$^{-/-}$ mice, the fraction of time spent in a spiking state was significantly reduced compared to the wild-type mice (Figure 4B), indicating a reduction in forebrain seizure activity in addition to the marked reduction in generalized seizures and death during status epilepticus.

BAD Manipulation Increases K_{ATP} Channel Activity

ATP-sensitive K^+ (K_{ATP}) channels are a well-known link between metabolism and cellular electrical activity. They are octamers comprised of four pore-forming Kir6.2 subunits and four modulatory SUR subunits and are inhibited by intracellular ATP (Nichols, 2006; Proks and Ashcroft, 2009; Yellen, 2008). These channels are expressed in many brain regions associated with epileptiform activity, such as the hippocampus (Dunn-Meynell et al., 1998; Karschin et al., 1997; Zawar et al., 1999). Additionally, K_{ATP} channel activity is increased when ketone bodies are applied to central neurons (Ma et al., 2007; Tanner et al., 2011).

To investigate a possible role of the K_{ATP} channel in mediating the seizure resistance of *Bad* mutant mice, we performed patch-clamp recordings in the cell-attached configuration from dentate

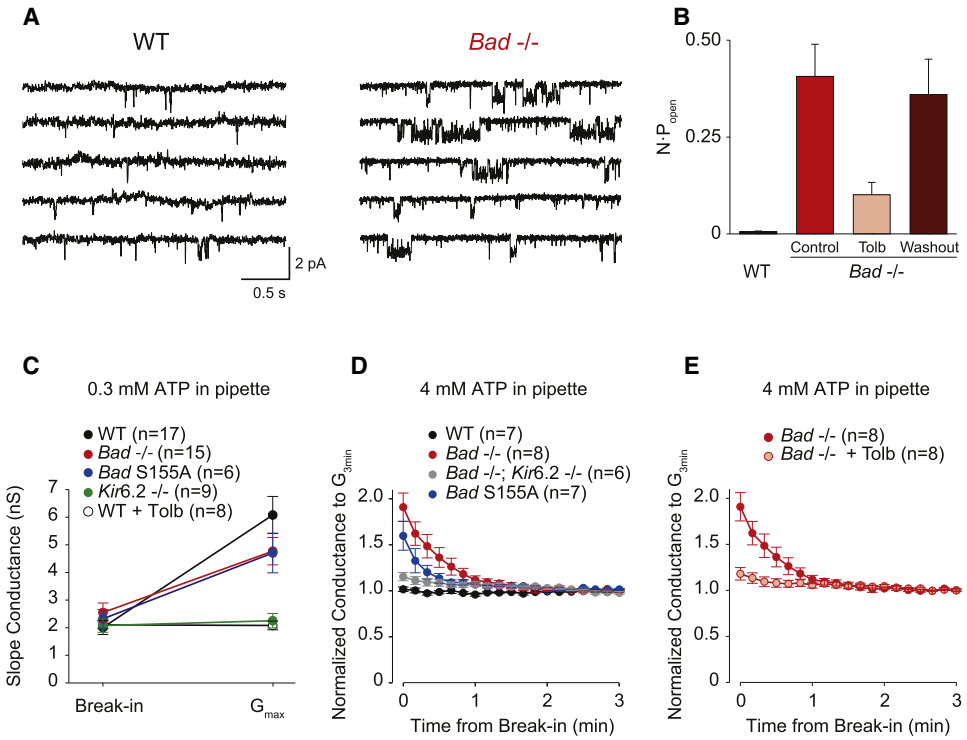

Figure 5. BAD Manipulations Increase K_{ATP} Channel Activity in Dentate Granule Neurons

(A) Continuous recordings of wild-type (left) or *Bad*$^{-/-}$ (right) single-channel currents in cell-attached patches with zero applied voltage. Single-channel openings are seen as downward deflections of the current trace.

(B) $N \cdot P_{open}$ values for WT and *Bad*$^{-/-}$ single channel recordings. For the *Bad*$^{-/-}$ recordings, the K_{ATP} blocker tolbutamide was added (Tolb; 200 μM) and then washed out (Washout). n = 6 for each genotype.

(C) Maximum activatable K_{ATP} conductance determined from the difference between the slope conductance at the time of break-in and after conductance run-up (G_{max}), with low ATP (0.3 mM) in the recording pipette, for the indicated genotypes and for WT in the presence of 200 μM tolbutamide (WT + Tolb).

(D) "Washdown" of an initially high K_{ATP} conductance, with high ATP (4 mM) in the recording pipette, seen in *Bad*$^{-/-}$ and *Bad* S155A but not in WT or in *Bad*$^{-/-}$; *Kir6.2*$^{-/-}$. The time course of slope conductance measured during whole-cell recording was normalized to the value 3 min after break-in.

(E) "Washdown" (measured as in D) prevented by preincubation in 200 μM tolbutamide. Data in (B) through (E) are presented as mean ± SEM.

See also Figure S6.

granule neurons (DGNs) in hippocampal slices, under recording conditions that block activity from most other channels (Tanner et al., 2011). The open probability (P_{open}) of single K_{ATP} channels was substantially increased in BAD-deficient neurons (Figures 5A and 5B). The highly active single channels measured in *Bad*$^{-/-}$ neurons were reversibly inhibited in the presence of 200 μM tolbutamide, a K_{ATP} channel inhibitor, thus confirming their identity (Figure 5B). These results indicate that, at the single channel level, the P_{open} of K_{ATP} channels is increased in *Bad* null mice.

We also tested the effect of BAD alteration on the total number of functional channels present in the cell membrane by measuring whole-cell K_{ATP} currents in DGNs. To measure the total activatable K_{ATP} conductance, we performed whole-cell recordings with reduced ATP (0.3 mM) in the pipette solution; in such experiments, K_{ATP} channels are disinhibited as the cellular contents exchange with the pipette. In wild-type, *Bad*$^{-/-}$ or *Bad*^{S155A} neurons, the cellular slope conductance increased to a maximum total activatable ("run-up") value within 10 min (Figure 5C) and the values were very similar for these three genotypes. As expected for a K_{ATP}-mediated current, current "run-up" was absent in *Kir6.2*$^{-/-}$ neurons or in wild-type neurons that were incubated in 200 μM tolbutamide prior to recording (Figure 5C).

To test for a whole-cell correlate of the high resting single channel P_{open} observed in cell-attached patches, we performed experiments with high ATP (4 mM) in the pipette, with the idea that as the ATP washes into the cell it might inhibit any initially active K_{ATP} channels. Indeed, we found that conductance in *Bad*$^{-/-}$ neurons decreased within the first minute after break-in with high ATP and then remained constant (Figure 5D). This "washdown" was not seen in wild-type cells (Figure 5D). It was also eliminated in *Bad*$^{-/-}$ neurons if they were preincubated with tolbutamide (Figure 5E) or in neurons from animals that lacked both BAD and Kir6.2 (Figure 5D), confirming that this initial high conductance was due to K_{ATP} channels. Current washdown also occurred in neurons from *Bad*^{S155A} mice (Figure 5D), showing that it is BAD's metabolic, rather than apoptotic, function that is responsible for increasing K_{ATP} conductance.

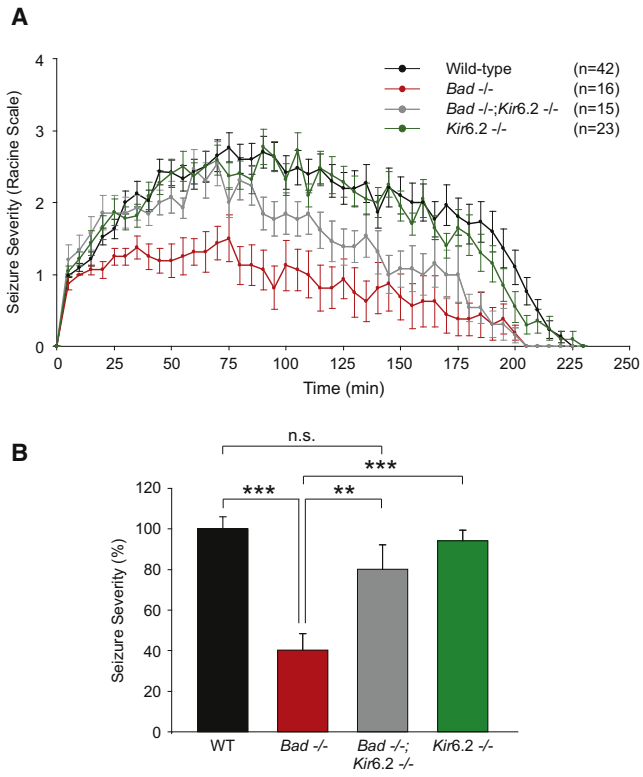

Figure 6. BAD Modulation of Seizure Resistance Is Dependent on the K_{ATP} Channel

(A and B) Raw scores (A) and seizure severity (B) in $Bad^{-/-}$ and $Kir6.2^{-/-}$ single mutants and $Bad^{-/-}$; $Kir6.2^{-/-}$ double mutant mice compared with wild-type mice after a single i.p. injection of kainic acid monitored and analyzed as in Figure 3. Data are presented as mean ± SEM. **p < 0.01; ***p < 0.001; n.s., nonsignificant; two-tailed Student's t test.

See also Figure S6.

BAD's Effect on KA-Induced Seizures Is Dependent on the K_{ATP} Channel

The marked increase in K_{ATP} channel open probability in $Bad^{-/-}$ DGNs suggests a link between K_{ATP} channel conductance and seizure protection in these mice and predicts that BAD's effect on seizure sensitivity may be mediated by the K_{ATP} channel. To test this prediction, we generated $Bad^{-/-}$; $Kir6.2^{-/-}$ double mutant mice and tested their sensitivity to KA in parallel with single $Bad^{-/-}$ or $Kir6.2^{-/-}$ mutants. Ablation of the Kir6.2 subunit in the *Bad* null genetic background substantially diminished the seizure resistance phenotype of $Bad^{-/-}$ mice (Figures 6A and 6B). Single deletion of the Kir6.2 subunit did not sensitize mice to acute seizures, arguing against an orthogonal or additive effect on seizures. These findings provide genetic evidence that the K_{ATP} channel is required for mediating BAD's effect on neuronal excitability.

DISCUSSION

Using a combination of genetic models and multiple experimental approaches ranging from mitochondrial respirometry in primary neural cultures and slice electrophysiology to behavioral and electrographic seizure monitoring in vivo, we provide a vertical analysis of BAD's effect on neural carbon substrate utilization, neuronal excitability, and seizure susceptibility. Our observations suggest that BAD imparts reciprocal effects on glucose and ketone body consumption through a phosphoregulatory mechanism that modifies S155 within its BH3 domain. Specifically, BAD deficiency or interference with its phosphorylation is associated with diminished mitochondrial metabolism of glucose and a concomitant metabolic preference for ketone bodies. An electrophysiologic consequence of this metabolic shift is a marked increase in the open probability of the metabolically sensitive K_{ATP} channel. Moreover, genetic studies indicate that this link between BAD-dependent programming of neural metabolism and neuronal excitability extends to reductions in electrographic and behavioral seizures, including the near absence of generalized tonic-clonic seizures. Importantly, BAD-dependent changes in seizure sensitivity are reversed by genetic modification of the Kir6.2 pore-forming subunit of the K_{ATP} channel, indicating that the K_{ATP} channel is a necessary downstream mediator of BAD's effect on neuronal excitation and seizure responses.

Several lines of evidence indicate that BAD modulation of sensitivity to acute seizures is distinct from alterations in the apoptotic pathway or a mere change in neuronal populations that might be expected from modification of a proapoptotic molecule. We have not found any evidence of neuronal loss in wild-type mice or *Bad* genetic models within the time course of acute seizures induced by i.p. delivery of KA (data not shown). Importantly, the shared seizure phenotype of *Bad* null and *Bad* S155A alleles that otherwise have opposite effects on BAD's apoptotic activity is consistent with the predominance of BAD's nonapoptotic properties in this setting. However, our findings do not argue against a role for apoptosis in epileptogenesis (Engel et al., 2011). Indeed, our experimental system of acute seizures is distinct from a chronic model of seizures induced by hippocampal damage 1–12 days after stereotactic delivery of KA in the amygdala (Engel et al., 2010; Murphy et al., 2010). In this model, loss of certain proapoptotic members of the BCL-2 family, such as BIM and PUMA, is protective against neuronal loss and brain damage associated with *status epilepticus*. However, ablation of *Bim* or *Puma* did not protect against acute seizures immediately after KA administration (Engel et al., 2010; Murphy et al., 2010). These observations are in agreement with our results that tissue-specific deletion of *Bim* in the brain does not alter the sensitivity to acute seizures (Figure S4).

Our findings are also distinct from previous reports suggesting a role for BAD in regulating synaptic transmission through modified recruitment/activation of proteins with known function in the regulation of the core apoptotic machinery, such as BAX, caspase-3, BCL-X_L, and VDAC (Hickman et al., 2008; Jiao and Li, 2011). Based on these studies, *Bad* null and Bad^{S155A} nonphosphorylatable mutants are predicted to exert opposite effects on the activity of these proteins. This is different from the shared phenotype of these BAD modifications in the neuronal activity we report here. Our results are instead consistent with involvement of BAD-dependent changes in

metabolism rather than modified components of the apoptotic machinery.

Metabolic changes similar to those produced by BAD manipulation have been found effective against epileptic seizures, notably, in the case of therapeutic diets, such as the KD. Reduced carbohydrate diets, such as the KD (Hartman et al., 2007; Neal et al., 2009; Thiele, 2003) and the low glycemic index treatment (Pfeifer et al., 2008; Pfeifer and Thiele, 2005), are effective against human epileptic seizures that are refractory to anticonvulsant drugs. These diets mimic fasting by reducing the carbohydrate supply and forcing the breakdown of fatty acids and utilization of ketone bodies as predominant carbon substrates. Whether it is reduced glucose metabolism per se, increased ketone body metabolism, or a combination of both that mediates seizure protection is under active investigation. However, this metabolic shift clearly reduces the incidence of seizures. In experimental animals, glycolytic inhibition can alter gene regulation and reduce epileptogenesis in a kindling model (Garriga-Canut et al., 2006; Stafstrom et al., 2009).

The reduced capacity to metabolize glucose and a simultaneous increase in the propensity to metabolize ketone bodies upon BAD modification is consistent with fuel competition (Hue and Taegtmeyer, 2009) and recapitulates the actual change in fuel consumption by the brain in fasting (Owen et al., 1967) or on KD (DeVivo et al., 1978). However, these BAD-dependent changes occur in the absence of dietary manipulation. Compared with systemic effects of dietary alterations, the seizure resistance in *Bad* null and S155A mice appears to likely arise from alterations in brain cell metabolism rather than systemic changes. In support of this idea, liver knockdown of *Bad* is not sufficient to produce seizure resistance (Figure S5) while it mimics the metabolic phenotype of the *Bad* null allele in the liver (data not shown). In addition, serum levels of circulating ketone bodies are not elevated in BAD-deficient mice under steady-state conditions (data not shown), thus it seems unlikely that changes in brain metabolism are driven by systemic changes.

The BAD-dependent metabolic shift can be demonstrated at the cellular level with changes in carbon substrate consumption in primary neuron or astrocyte cultures, consistent with cell-autonomous metabolic effects of BAD. These metabolic changes have the consequence of elevating the open probability of K_{ATP} channels, as seen in both whole-cell and cell-attached recordings from DGNs in brain slices. Either glucose deprivation or ketone body metabolism can produce elevated K_{ATP} channel activity, and these effects can be augmented by increased neuronal firing (Ma et al., 2007; Tanner et al., 2011), as seen during seizures. The exact mechanism of K_{ATP} channel activation by BAD-dependent metabolic changes is not known; changes in ATP and ADP are a possible mechanism, though other metabolites, such as PIP_2, are also known to regulate the activity of K_{ATP} channels (Nichols, 2006), and we cannot rule out changes in the properties of the channel through some unknown signal resulting from genetic alteration of *Bad*. Total cellular ATP levels and the ATP/ADP ratio in whole brain under steady-state conditions are comparable in WT and $Bad^{-/-}$ brains (Figures S6A and S6B). However, these measurements may not reflect the dynamic fluctuations that occur during seizures or local changes that could contribute to the increased activity of the K_{ATP} channel. Remarkably, the whole brain content of β-hydroxybutyrate is significantly higher in $Bad^{-/-}$ mice compared with controls (Figure S6C). As ketone bodies can increase the activity of the K_{ATP} channel in central neurons (Ma et al., 2007; Tanner et al., 2011), their higher content in $Bad^{-/-}$ brain may provide, at least in part, a link to the observed increase in K_{ATP} channel activity. Interestingly, although the whole brain content of ketone bodies in $Bad^{-/-}$ mice is elevated, the serum level of these metabolites are unaltered (data not shown), suggesting local changes in ketone body generation and handling.

The observed increase in K_{ATP} activity in dentate granule neurons indicates one way in which BAD induced metabolic changes might lead to seizure resistance. The dentate gyrus, where DGNs are located, has been hypothesized to be one of the regions of the brain capable of functioning as a "seizure gate" (Brenner et al., 2005; Coulter, 1999; Heinemann et al., 1992; Hsu, 2007). However, these neurons are only one of the many types of central neurons that express K_{ATP} channels (Dunn-Meynell et al., 1998; Inagaki et al., 1996; Karschin et al., 1997; Zawar et al., 1999), and important effects may also arise elsewhere.

In addition to the observation that K_{ATP} activity is augmented in the *Bad* genetic models, the near complete reversal of the seizure resistance in *Bad* null mice with genetic ablation of the Kir6.2 subunit of the K_{ATP} channel provides strong genetic evidence for the BAD-K_{ATP} axis in modulation of seizure susceptibility. Although the genetic data underscore the K_{ATP} channel as a mechanistic component of BAD's effect in this setting, they do not rule out contribution from additional consequences of a glucose-to-ketone-body metabolic shift.

Our findings reveal BAD as a novel molecular player in the metabolic control of neuronal excitation that imparts robust changes in susceptibility to both behavioral and electrographic seizures. BAD's capacity to modulate the neural choice of carbon substrate and energy metabolism in the brain, independent of dietary manipulation, makes it an attractive candidate for metabolic manipulation of seizure responses. Small molecules modeled after BAD variants that promote ketone body catabolism over glucose metabolism may help uncover new therapeutic targets to treat epileptic disorders.

EXPERIMENTAL PROCEDURES

Animals

$Bad^{-/-}$ and Bad^{S155A} knockin mice have been previously described (Danial et al., 2008). *Bad* genetic models used in this study were bred into the C57BL/6J genetic background for at least 14 generations and were validated by genome scanning to be 99.9% congenic with C57BL/6J. $Bid^{-/-}$, $Bim^{F/F}$, and $Kir6.2^{-/-}$, mice have been previously described (Miki et al., 1998; Takeuchi et al., 2005; Yin et al., 1999). *Nestin*-CRE mice were purchased from Jackson Laboratory (Bar Harbor, ME, USA). Mice received a standard chow diet and were housed in a barrier facility with 12 hr light and dark cycles. All animal procedures were approved by the Institutional Animal Care and Use Committee of Dana-Farber Cancer Institute and Harvard Medical School. Cohorts of 8- to 10-week-old male mice were used in all in vivo studies.

Kainic Acid Treatment and Monitoring of Behavioral Seizures

Kainic acid (KA; Tocris Bioscience, MO, USA) was dissolved in saline (Sigma-Aldrich, St. Louis, MO, USA) and injected intraperitoneally (i.p.) at a dose of

30 mg/kg of body weight. Behavioral seizures in mice were scored every 5 min for up to 4 hr in accordance with a modified version of the Racine scale as previously described (Ferraro et al., 1997). Briefly, the modified Racine scale includes four stages:

Stage 1. Hypoactivity: rigidity, immobility, or crawling, fixed gaze, and postural abnormalities, including hunched posture.
Stage 2. Partial clonus: behavioral seizure activity affecting mostly the head (grimacing, twitching, and head nodding) and/or forelimbs(s) ("paddling"). Rigidity.
Stage 3. Generalized clonus: loss of upright posture, whole body clonus, rearing, wild running and jumping, and autonomic signs. Fore- and hindlimb extension.
Stage 4. Status epilepticus: severe clonic-tonic convulsions. Complete loss of balance and control.

Seizure severity was scored by an investigator blind to the genotype. In addition to recording raw seizure scores, seizure severity was determined by integrating individual scores per mouse over the duration of the experiment using the following formula:

$$\text{Seizure Severity} = \sum(\text{all scores of a given mouse})/\text{time of experiment}.$$

All scores for a single mouse were added and then divided by the total time of the experiment for each animal. The mean of the seizure severity values from wild-type mice was assigned a value of "100." This value was then used to normalize the severity of the other tested genotypes within the same scale. This formula provided better accounting for seizure severity in mice that died during the experiment.

Pentylenetetrazole Treatment and Monitoring of Behavioral Seizures

Mice were injected subcutaneously (s.c.) with pentylenetetrazole (PTZ; Sigma-Aldrich) dissolved in saline at a final dose of 80 mg/kg of body weight as previously described (Ferraro et al., 1999). Behavioral seizures were scored every 2.5 min up to 80 min in accordance with a modified version of the Racine scale as detailed previously.

Electroencephalographic Recording

Mice were anesthetized with a mixture of ketamine/xylazine at a dose of 120 and 12 mg/kg of body weight, respectively. Headmounts for EEG recordings (8200 Series, 3 channel-2 EEG/1 EMG for mice, Pinnacle Technology, Inc., KS, USA) were then placed by stereotactic surgery per the manufacturer's instructions. Mice were allowed to recover for 5–7 days. After recovery, a Pinnacle preamplifier was plugged in the headmount, and the mouse was then placed in an open plexiglas recording cage with wires connected via a swivel to the digitizer. Data were acquired using the PAL 8200 software (Pinnacle Technology, Inc.) at a sample rate of 400 Hz.

EEG data were analyzed in MATLAB using the BIOSIG-toolbox (http://biosig.sf.net) and specially written browsing and analysis software. In addition to displaying the raw EEG and EMG traces, power in the 20–70 Hz band was calculated using a fifth-order Butterworth bandpass filter (Lehmkuhle et al., 2009) and measured relative to the baseline period to help identify onset and offset of high-energy spiking. EEGs were scored by an investigator blind to the genotype, and the fraction of time spent in a high-energy spiking state was determined for a 30 min period beginning 3 min after KA injection.

Primary Cultures of Neurons and Astrocytes

Primary cortical neurons were cultured in accordance with an established protocol with some modifications (Banker and Goslin, 1998). Seventeen-day-old embryos were dissected in prechilled Hank's buffered salt solution (HBSS). After removal of the meninges, striatum, and hippocampus, the intact cortices were washed in Ca^{2+} and Mg^{2+}-free HBSS, cut into small pieces and incubated in a Ca^{2+} and Mg^{2+}-free HBSS solution containing 0.25% trypsin (Sigma-Aldrich) and 1 mg/ml DNaseI (Roche Diagnostics, Indianapolis, IN, USA) for 15 min at 37°C with gentle shaking every 3–4 min. The dissociated cells were then resuspended and plated in minimum essential medium supplemented with 0.6% glucose and 10% horse serum (Invitrogen, Carlsbad, CA, USA). The medium was changed after 4 hr to Neurobasal culture medium supplemented with B-27, 2 mM GlutaMaxI (all from Invitrogen), and a mix of penicillin and streptomycin (100 U/ml and 100 μg/ml, respectively). The cells were plated at 3×10^5 cells/cm^2 on poly-L-lysine precoated plates and fed every 3 days by replacing one-third of the medium with fresh media. Cells were cultured 5–6 days prior to experiments.

Primary cortical astrocytes were obtained from 1-day-old newborn mouse pups and processed as above. The cells were seeded on poly-L-lysine-coated plates in a mixture of Dulbecco's modified Eagle's medium (DMEM) + HAMs F-12 nutrient mixture (1:1) supplemented with 10% fetal bovine serum (FBS; Invitrogen), 2 mM GlutaMaxI, and a mix of penicillin and streptomycin (100 U/ml and 100 μg/ml, respectively) and cultured for 2–3 weeks but no more than two passages. This ensured homogeneity of the primary cultures prior to mitochondrial respirometry assays.

Assessment of Oxygen Consumption Rate

Real-time measurement of mitochondrial oxygen consumption rate (OCR) and data processing were carried out using the XF24 extracellular flux analyzer instrument and the AKOS algorithm built in the XF24 v1.7.0.74 software (Seahorse Bioscience, Inc., Billerica, MA, USA; Wu et al., 2007). Primary neurons were seeded on poly-L-lysine-coated XF24 V7 plates at 1×10^5 cells/well and incubated for 5–6 days before OCR measurements. Primary astrocytes were seeded on poly-L-lysine-coated XF24 V7 plates at 4×10^4 cells/well and allowed to recover overnight. On the day of the experiment, the cells were rinsed once in DMEM without sodium bicarbonate (Sigma-Aldrich) and preincubated for 1 hr in sodium bicarbonate-free DMEM supplemented with the carbon substrate to be tested (10 mM D-glucose, 5 mM β-D-hydroxybutyrate, 5 mM L-lactate, or 5 mM L-glutamine). For neurons, the media was additionally supplemented with B-27.

After baseline measurements, maximal mitochondrial maximal respiration (MR) in response to a given substrate was determined following the addition of the uncoupler carbonyl cyanide 4-(trifluoromethoxy) phenylhydrazone (FCCP, Sigma-Aldrich) at 1 and 0.5 μM final concentration to neurons and astrocytes, respectively. OCR was then recorded until it reached a plateau. The fraction of OCR that is due to mitochondrial respiration was determined by subsequent addition of the mitochondrial complex I inhibitor rotenone (Sigma-Aldrich) at 1 μM. MR was derived from the difference between maximal respiratory rate induced by FCCP and the lowest respiratory rate after rotenone treatment.

Hippocampal Slice Preparation for Patch-Clamp Recordings

Acute hippocampal slices 400 μm thick were cut in the transverse plane from the brains of 12- to 18-day-old mice, using a vibrating tissue slicer (Vibratome, St. Louis, MO, USA). Mice were anesthetized by isoflurane inhalation and decapitated into an ice-cold slurry containing the following (in mM): 87 NaCl, 25 $NaHCO_3$, 25 D-glucose, 75 sucrose, 2.5 KCl, 1.25 NaH_2PO_4, 0.5 $CaCl_2$, and 7 $MgCl_2$ (osmolality 340 mmol/kg; pH 7.4 with NaOH). Slices were incubated at 37°C for 20 min in the slicing solution and then for 40 min in recording solution and then stored at room temperature for 0–3 hr before use. During recording, ACSF was delivered to the bath using a peristaltic pump at a flow rate of 1 ml/min. All ACSF solutions for whole-cell and single-channel recordings contained the following (in mM): 120 NaCl, 26 $NaHCO_3$, 10 D-glucose, 2.5 KCl, 2 $CaCl_2$, 1.25 NaH_2PO_4, and 1 $MgCl_2$ (osmolality 300 mmol/kg; pH 7.4). In addition, all recording solutions contained 100 μM picrotoxin and 1 mM kynurenic acid to block fast synaptic transmission. All bath solutions were bubbled continuously with 95% O_2 and 5% CO_2. All chemicals were purchased from Sigma-Aldrich.

Patch-Clamp Recordings

Cell-attached patch recordings from individual dentate granule neurons identified under infrared differential interference contrast (IR-DIC) visual guidance were made in voltage-clamp mode following establishment of high-resistance (multi-GΩ) seals. Data were collected with a HEKA EPC 10 patch-clamp amplifier (HEKA Instruments Inc., Bellmore, NY, USA). Macroscopic and single-

channel currents were filtered at 1 kHz and sampled at 10 kHz. Patchmaster v2x43 software (HEKA Instruments Inc.) was used for amplifier control and data acquisition. All recordings were obtained at room temperature. Patch pipettes were pulled from borosilicate glass (VWR Scientific or Dagan LG16 for macroscopic or single-channel current recordings, respectively) using a Sutter Instruments P-97 puller. Pipette tips were fire polished to resistances of 2–3 MΩ when filled with recording solutions.

For cell-attached recordings, the pipette solution contained (in mM): 140 potassium methanesulfonate (KMeS), 10 HEPES, 2 $CaCl_2$, and 10 TEA-Cl, 2 CsCl, 1 4-aminopyridine (4-AP), 100 nM charybdotoxin (in 0.001% BSA; Alomone Labs, Jerusalem, Israel), and 100 nM apamin (including 40 μM acetic acid; EMD Millipore, Billerica, MA, USA) to block non-K_{ATP} potassium channels (osmolality 310 mmol/kg; pH to 7.4 with KOH). Peptide blockers were stored as stocks at −20°C and diluted prior to recording.

For whole-cell recordings, the pipette solution contained (in mM): 140 KMeS, 10 NaCl, 10 HEPES, 1 $MgCl_2$, and 0.1 EGTA (osmolality 295 mmol/kg; pH 7.4), supplemented with 0.3 mM Na_3GTP and either 0.3 or 4 mM MgATP. A voltage ramp protocol was used to measure input resistance and slope conductance: from the −90 mV holding potential followed two 100 ms steps first to −100 mV then to −120 mV before initiation of a 1 s ramp from −120 to −65 mV. The prepulses were used to calculate the cell's input resistance. Voltage ramps were applied every 10 s and fitted with a straight line from −120 to −80 mV to provide a running assessment of whole-cell slope conductance.

Tolbutamide was diluted in ACSF from a 200 mM stock solution in ethanol. Ethanol as a vehicle control was added to ACSF at 0.1%. All chemicals are from Sigma-Aldrich, unless otherwise noted.

Patch-Clamp Data Analysis

Data and statistical analysis were performed with Patchmaster v2x43 (HEKA Instruments Inc.) and Origin 8 (OriginLab, Northampton, MA, USA). Single-channel analysis was performed using QuB (http://www.qub.buffalo.edu). Open and closed levels for channel activity were detected using a 50% threshold criterion. Raw data sets featuring excessive baseline shift, sufficient high- or low-frequency noise to preclude effective idealization of channel openings, or too few data traces (<3 min of recording) were discarded without idealization or further analysis. The number of independent experiments (n, Figure 5) corresponds to the number of patches or whole-cell experiments each from a different hippocampal slice. In all cases, each experimental condition was tested in slices from at least three different animals.

Statistical Analysis

In all cases, mean ± SEM is presented. The number of independent experiments is indicated in the figure or figure legend in each case. Statistical significance was determined using two-tailed Student's t test.

SUPPLEMENTAL INFORMATION

Supplemental Information includes six figures and Supplemental Experimental Procedures and can be found with this article online at doi:10.1016/j.neuron.2012.03.032.

ACKNOWLEDGMENTS

We thank Marina Godes and Juan Quijada for technical assistance and animal husbandry; Gregory Holmes for advice on EEG acquisition and analysis; Rosalind Segal, Bernardo Sabatini, Qiufu Ma, S. Robert Datta, and members of the Danial and Yellen laboratories for critical reading of this manuscript and valuable discussions; and E. Smith for manuscript preparation. A.G.C. was supported by a postdoctoral fellowship from the Ministerio de Educación y Ciencia (MEC, Spain). N.N.D. is a recipient of the Burroughs Wellcome Fund Career Award in Biomedical Sciences. This work was supported by the U.S. National Institutes of Health grants (K01CA106596 to N.N.D., R01 NS055031 to G.Y., and R56 NS072142 to N.N.D. and G.Y.), Harvard Catalyst Pilot Award (based on NIH UL1 RR025758 to N.N.D. and G.Y.), and a CURE Epilepsy Challenge Award (G.Y. and N.N.D.).

Accepted: March 8, 2012
Published: May 24, 2012

REFERENCES

Banker, G., and Goslin, K. (1998). Culturing Nerve Cells, Second Edition (Cambridge, MA: MIT Press).

Ben-Ari, Y., Tremblay, E., Ottersen, O.P., and Meldrum, B.S. (1980). The role of epileptic activity in hippocampal and "remote" cerebral lesions induced by kainic acid. Brain Res. *191*, 79–97.

Bough, K.J., and Eagles, D.A. (1999). A ketogenic diet increases the resistance to pentylenetetrazole-induced seizures in the rat. Epilepsia *40*, 138–143.

Brand, M.D., and Nicholls, D.G. (2011). Assessing mitochondrial dysfunction in cells. Biochem. J. *435*, 297–312.

Brenner, R., Chen, Q.H., Vilaythong, A., Toney, G.M., Noebels, J.L., and Aldrich, R.W. (2005). BK channel beta4 subunit reduces dentate gyrus excitability and protects against temporal lobe seizures. Nat. Neurosci. *8*, 1752–1759.

Browning, R.A. (1994). Anatomy of Generalized Convulsive Seizures. In Idiopathic Generalized Epilepsies: Clinical, Experimental and Genetic Aspects, A. Malafosse, P. Genton, E. Hirsch, C. Marescaux, D. Broglin, and R. Bernasconi, eds. (London: Libbey), pp. 399–414.

Browning, R.A., Wang, C., Lanker, M.L., and Jobe, P.C. (1990). Electroshock- and pentylenetetrazol-induced seizures in genetically epilepsy-prone rats (GEPRs): differences in threshold and pattern. Epilepsy Res. *6*, 1–11.

Coulter, D.A. (1999). Chronic epileptogenic cellular alterations in the limbic system after status epilepticus. Epilepsia *40*, S23–S33.

Chipuk, J.E., Moldoveanu, T., Llambi, F., Parsons, M.J., and Green, D.R. (2010). The BCL-2 family reunion. Mol. Cell *37*, 299–310.

Dahlin, M., Elfving, A., Ungerstedt, U., and Amark, P. (2005). The ketogenic diet influences the levels of excitatory and inhibitory amino acids in the CSF in children with refractory epilepsy. Epilepsy Res. *64*, 115–125.

Danial, N.N. (2008). BAD: undertaker by night, candyman by day. Oncogene *27* (*Suppl 1*), S53–S70.

Danial, N.N., and Korsmeyer, S.J. (2004). Cell death: critical control points. Cell *116*, 205–219.

Danial, N.N., Gramm, C.F., Scorrano, L., Zhang, C.Y., Krauss, S., Ranger, A.M., Datta, S.R., Greenberg, M.E., Licklider, L.J., Lowell, B.B., et al. (2003). BAD and glucokinase reside in a mitochondrial complex that integrates glycolysis and apoptosis. Nature *424*, 952–956.

Danial, N.N., Walensky, L.D., Zhang, C.Y., Choi, C.S., Fisher, J.K., Molina, A.J., Datta, S.R., Pitter, K.L., Bird, G.H., Wikstrom, J.D., et al. (2008). Dual role of proapoptotic BAD in insulin secretion and beta cell survival. Nat. Med. *14*, 144–153.

Datta, S.R., Katsov, A., Hu, L., Petros, A., Fesik, S.W., Yaffe, M.B., and Greenberg, M.E. (2000). 14-3-3 proteins and survival kinases cooperate to inactivate BAD by BH3 domain phosphorylation. Mol. Cell *6*, 41–51.

DeVivo, D.C., Leckie, M.P., Ferrendelli, J.S., and McDougal, D.B., Jr. (1978). Chronic ketosis and cerebral metabolism. Ann. Neurol. *3*, 331–337.

Dunn-Meynell, A.A., Rawson, N.E., and Levin, B.E. (1998). Distribution and phenotype of neurons containing the ATP-sensitive K^+ channel in rat brain. Brain Res. *814*, 41–54.

Engel, T., Hatazaki, S., Tanaka, K., Prehn, J.H., and Henshall, D.C. (2010). Deletion of Puma protects hippocampal neurons in a model of severe status epilepticus. Neuroscience *168*, 443–450.

Engel, T., Plesnila, N., Prehn, J.H., and Henshall, D.C. (2011). In vivo contributions of BH3-only proteins to neuronal death following seizures, ischemia, and traumatic brain injury. J. Cereb. Blood Flow Metab. *31*, 1196–1210.

Fern, R. (2003). Variations in spare electron transport chain capacity: The answer to an old riddle? J. Neurosci. Res. *71*, 759–762.

Ferraro, T.N., Golden, G.T., Smith, G.G., Schork, N.J., St Jean, P., Ballas, C., Choi, H., and Berrettini, W.H. (1997). Mapping murine loci for seizure response to kainic acid. Mamm. Genome *8*, 200–208.

Ferraro, T.N., Golden, G.T., Smith, G.G., St Jean, P., Schork, N.J., Mulholland, N., Ballas, C., Schill, J., Buono, R.J., and Berrettini, W.H. (1999). Mapping loci for pentylenetetrazol-induced seizure susceptibility in mice. J. Neurosci. *19*, 6733–6739.

Garriga-Canut, M., Schoenike, B., Qazi, R., Bergendahl, K., Daley, T.J., Pfender, R.M., Morrison, J.F., Ockuly, J., Stafstrom, C., Sutula, T., and Roopra, A. (2006). 2-Deoxy-D-glucose reduces epilepsy progression by NRSF-CtBP-dependent metabolic regulation of chromatin structure. Nat. Neurosci. *9*, 1382–1387.

Hartman, A.L., Gasior, M., Vining, E.P., and Rogawski, M.A. (2007). The neuropharmacology of the ketogenic diet. Pediatr. Neurol. *36*, 281–292.

Haugvicová, R., Kubová, H., Skutová, M., and Mares, P. (2000). Anticonvulsant action of topiramate against motor seizures in developing rats. Epilepsia *41*, 1235–1240.

Heinemann, U., Beck, H., Dreier, J.P., Ficker, E., Stabel, J., and Zhang, C.L. (1992). The dentate gyrus as a regulated gate for the propagation of epileptiform activity. Epilepsy Res. Suppl. *7*, 273–280.

Hickman, J.A., Hardwick, J.M., Kaczmarek, L.K., and Jonas, E.A. (2008). Bcl-xL inhibitor ABT-737 reveals a dual role for Bcl-xL in synaptic transmission. J. Neurophysiol. *99*, 1515–1522.

Hsu, D. (2007). The dentate gyrus as a filter or gate: a look back and a look ahead. Prog. Brain Res. *163*, 601–613.

Hue, L., and Taegtmeyer, H. (2009). The Randle cycle revisited: a new head for an old hat. Am. J. Physiol. Endocrinol. Metab. *297*, E578–E591.

Inagaki, N., Gonoi, T., Clement, J.P., Wang, C.Z., Aguilar-Bryan, L., Bryan, J., and Seino, S. (1996). A family of sulfonylurea receptors determines the pharmacological properties of ATP-sensitive K^+ channels. Neuron *16*, 1011–1017.

Jarrett, S.G., Milder, J.B., Liang, L.P., and Patel, M. (2008). The ketogenic diet increases mitochondrial glutathione levels. J. Neurochem. *106*, 1044–1051.

Jeong, E.A., Jeon, B.T., Shin, H.J., Kim, N., Lee, D.H., Kim, H.J., Kang, S.S., Cho, G.J., Choi, W.S., and Roh, G.S. (2011). Ketogenic diet-induced peroxisome proliferator-activated receptor-γ activation decreases neuroinflammation in the mouse hippocampus after kainic acid-induced seizures. Exp. Neurol. *232*, 195–202.

Jiao, S., and Li, Z. (2011). Nonapoptotic function of BAD and BAX in long-term depression of synaptic transmission. Neuron *70*, 758–772.

Juge, N., Gray, J.A., Omote, H., Miyaji, T., Inoue, T., Hara, C., Uneyama, H., Edwards, R.H., Nicoll, R.A., and Moriyama, Y. (2010). Metabolic control of vesicular glutamate transport and release. Neuron *68*, 99–112.

Karschin, C., Ecke, C., Ashcroft, F.M., and Karschin, A. (1997). Overlapping distribution of K_{ATP} channel-forming Kir6.2 subunit and the sulfonylurea receptor SUR1 in rodent brain. FEBS Lett. *401*, 59–64.

Klitgaard, H., Matagne, A., Gobert, J., and Wülfert, E. (1998). Evidence for a unique profile of levetiracetam in rodent models of seizures and epilepsy. Eur. J. Pharmacol. *353*, 191–206.

Lehmkuhle, M.J., Thomson, K.E., Scheerlinck, P., Pouliot, W., Greger, B., and Dudek, F.E. (2009). A simple quantitative method for analyzing electrographic status epilepticus in rats. J. Neurophysiol. *101*, 1660–1670.

Ma, W., Berg, J., and Yellen, G. (2007). Ketogenic diet metabolites reduce firing in central neurons by opening K_{ATP} channels. J. Neurosci. *27*, 3618–3625.

MacAskill, A.F., Atkin, T.A., and Kittler, J.T. (2010). Mitochondrial trafficking and the provision of energy and calcium buffering at excitatory synapses. Eur. J. Neurosci. *32*, 231–240.

Masino, S.A., Li, T., Theofilas, P., Sandau, U.S., Ruskin, D.N., Fredholm, B.B., Geiger, J.D., Aronica, E., and Boison, D. (2011). A ketogenic diet suppresses seizures in mice through adenosine A_1 receptors. J. Clin. Invest. *121*, 2679–2683.

Miki, T., Nagashima, K., Tashiro, F., Kotake, K., Yoshitomi, H., Tamamoto, A., Gonoi, T., Iwanaga, T., Miyazaki, J., and Seino, S. (1998). Defective insulin secretion and enhanced insulin action in K_{ATP} channel-deficient mice. Proc. Natl. Acad. Sci. USA *95*, 10402–10406.

Murphy, B.M., Engel, T., Paucard, A., Hatazaki, S., Mouri, G., Tanaka, K., Tuffy, L.P., Jimenez-Mateos, E.M., Woods, I., Dunleavy, M., et al. (2010). Contrasting patterns of Bim induction and neuroprotection in Bim-deficient mice between hippocampus and neocortex after status epilepticus. Cell Death Differ. *17*, 459–468.

Neal, E.G., Chaffe, H., Schwartz, R.H., Lawson, M.S., Edwards, N., Fitzsimmons, G., Whitney, A., and Cross, J.H. (2009). A randomized trial of classical and medium-chain triglyceride ketogenic diets in the treatment of childhood epilepsy. Epilepsia *50*, 1109–1117.

Nichols, C.G. (2006). K_{ATP} channels as molecular sensors of cellular metabolism. Nature *440*, 470–476.

Nicholls, D.G. (2009). Mitochondrial calcium function and dysfunction in the central nervous system. Biochim. Biophys. Acta *1787*, 1416–1424.

Noh, H.S., Kim, Y.S., Lee, H.P., Chung, K.M., Kim, D.W., Kang, S.S., Cho, G.J., and Choi, W.S. (2003). The protective effect of a ketogenic diet on kainic acid-induced hippocampal cell death in the male ICR mice. Epilepsy Res. *53*, 119–128.

Owen, O.E., Morgan, A.P., Kemp, H.G., Sullivan, J.M., Herrera, M.G., and Cahill, G.F., Jr. (1967). Brain metabolism during fasting. J. Clin. Invest. *46*, 1589–1595.

Pfeifer, H.H., and Thiele, E.A. (2005). Low-glycemic-index treatment: a liberalized ketogenic diet for treatment of intractable epilepsy. Neurology *65*, 1810–1812.

Pfeifer, H.H., Lyczkowski, D.A., and Thiele, E.A. (2008). Low glycemic index treatment: implementation and new insights into efficacy. Epilepsia *49*, 42–45.

Proks, P., and Ashcroft, F.M. (2009). Modeling K_{ATP} channel gating and its regulation. Prog. Biophys. Mol. Biol. *99*, 7–19.

Schwartzkroin, P.A. (1999). Mechanisms underlying the anti-epileptic efficacy of the ketogenic diet. Epilepsy Res. *37*, 171–180.

Stafstrom, C.E., and Rho, J.M. (2004). Epilepsy and the Ketogenic Diet (Totowa, NJ: Humana Press).

Stafstrom, C.E., Ockuly, J.C., Murphree, L., Valley, M.T., Roopra, A., and Sutula, T.P. (2009). Anticonvulsant and antiepileptic actions of 2-deoxy-D-glucose in epilepsy models. Ann. Neurol. *65*, 435–447.

Takeuchi, O., Fisher, J., Suh, H., Harada, H., Malynn, B.A., and Korsmeyer, S.J. (2005). Essential role of BAX,BAK in B cell homeostasis and prevention of autoimmune disease. Proc. Natl. Acad. Sci. USA *102*, 11272–11277.

Tanner, G.R., Lutas, A., Martínez-François, J.R., and Yellen, G. (2011). Single K_{ATP} channel opening in response to action potential firing in mouse dentate granule neurons. J. Neurosci. *31*, 8689–8696.

Thiele, E.A. (2003). Assessing the efficacy of antiepileptic treatments: the ketogenic diet. Epilepsia *44* (*Suppl 7*), 26–29.

Velíšková, J. (2005). Behavioral Characterization of Seizures in Rats. In Models of Seizures and Epilepsy, A. Pitkänen, P.A. Schwartzkroin, and S. Moshé, eds. (Burlington, MA: Elsevier Academic Press), pp. 601–611.

Wang, Z.J., Bergqvist, C., Hunter, J.V., Jin, D., Wang, D.J., Wehrli, S., and Zimmerman, R.A. (2003). In vivo measurement of brain metabolites using two-dimensional double-quantum MR spectroscopy—exploration of GABA levels in a ketogenic diet. Magn. Reson. Med. *49*, 615–619.

Wu, M., Neilson, A., Swift, A.L., Moran, R., Tamagnine, J., Parslow, D., Armistead, S., Lemire, K., Orrell, J., Teich, J., et al. (2007). Multiparameter metabolic analysis reveals a close link between attenuated mitochondrial bioenergetic function and enhanced glycolysis dependency in human tumor cells. Am. J. Physiol. Cell Physiol. *292*, C125–C136.

Yellen, G. (2008). Ketone bodies, glycolysis, and K_{ATP} channels in the mechanism of the ketogenic diet. Epilepsia *49* (*Suppl 8*), 80–82.

Yin, X.M., Wang, K., Gross, A., Zhao, Y., Zinkel, S., Klocke, B., Roth, K.A., and Korsmeyer, S.J. (1999). Bid-deficient mice are resistant to Fas-induced hepatocellular apoptosis. Nature *400*, 886–891.

Youle, R.J., and Strasser, A. (2008). The BCL-2 protein family: opposing activities that mediate cell death. Nat. Rev. Mol. Cell Biol. *9*, 47–59.

Yudkoff, M., Daikhin, Y., Nissim, I., Lazarow, A., and Nissim, I. (2001). Ketogenic diet, amino acid metabolism, and seizure control. J. Neurosci. Res. *66*, 931–940.

Zawar, C., Plant, T.D., Schirra, C., Konnerth, A., and Neumcke, B. (1999). Cell-type specific expression of ATP-sensitive potassium channels in the rat hippocampus. J. Physiol. *514*, 327–341.

Zielke, H.R., Zielke, C.L., and Baab, P.J. (2009). Direct measurement of oxidative metabolism in the living brain by microdialysis: a review. J. Neurochem. *109* (*Suppl 1*), 24–29.

Ziemann, A.E., Schnizler, M.K., Albert, G.W., Severson, M.A., Howard, M.A., 3rd, Welsh, M.J., and Wemmie, J.A. (2008). Seizure termination by acidosis depends on ASIC1a. Nat. Neurosci. *11*, 816–822.

Neuron, volume *74*

Supplemental Information

BAD-Dependent Regulation of Fuel Metabolism and K_{ATP} Channel Activity Confers Resistance to Epileptic Seizures

Alfredo Giménez-Cassina, Juan Ramón Martínez-François, Jill K. Fisher, Benjamin Szlyk, Klaudia Polak, Jessica Wiwczar, Geoffrey R. Tanner, Andrew Lutas, Gary Yellen and Nika N. Danial

This file contains six Supplemental Figures and Legends, Supplemental Experimental Procedures, and Supplemental References.

SUPPLEMENTAL FIGURES AND LEGENDS

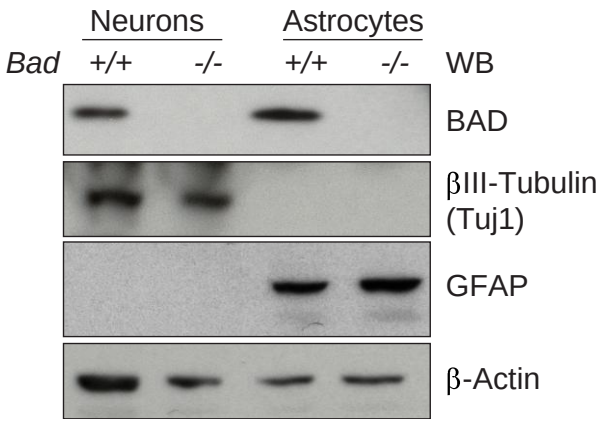

Figure S1, related to Figure 1. BAD Expression in Primary Cortical Neurons and Astrocytes. Western blot of primary neurons and astrocytes derived from wild-type and *Bad* $^{-/-}$ mice. The neuronal marker βIII-tubulin (Tuj1) and glial marker glial-fibrillary acidic protein GFAP levels serve as quality control for the purity of the neurons and astrocyte cultures, respectively. β-actin was used as loading control.

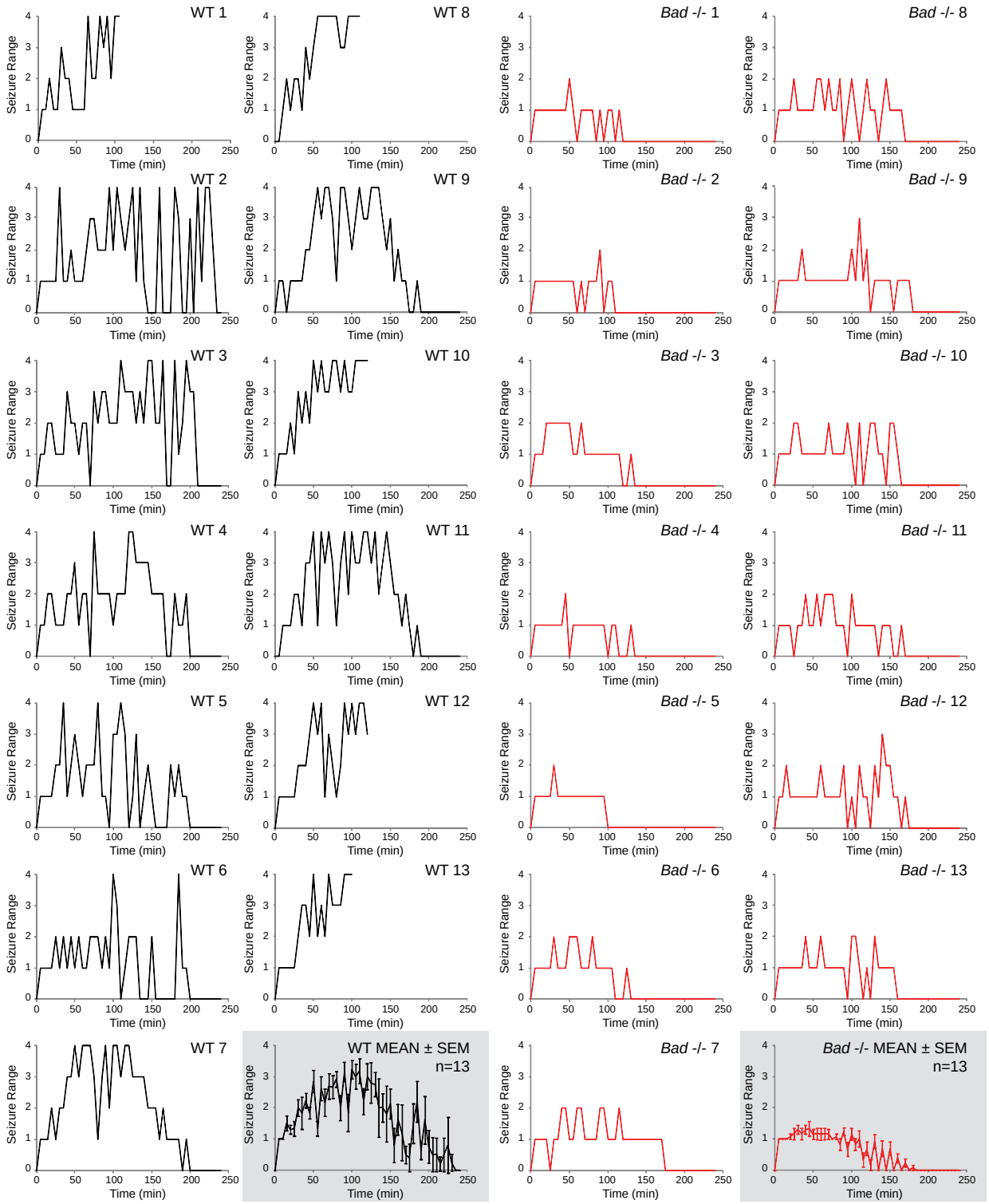

Figure S2, related to Figure 3. Seizure Diaries for Individual Mice. Diaries in black (two columns of panels on the left) correspond to WT mice and those in red (two columns of panels on the right) correspond to *Bad* $^{-/-}$ mice (n=13 per genotype). The average scores of all the mice per genotype as depicted in Figure 3 is also included in two bottom panels shaded in grey.

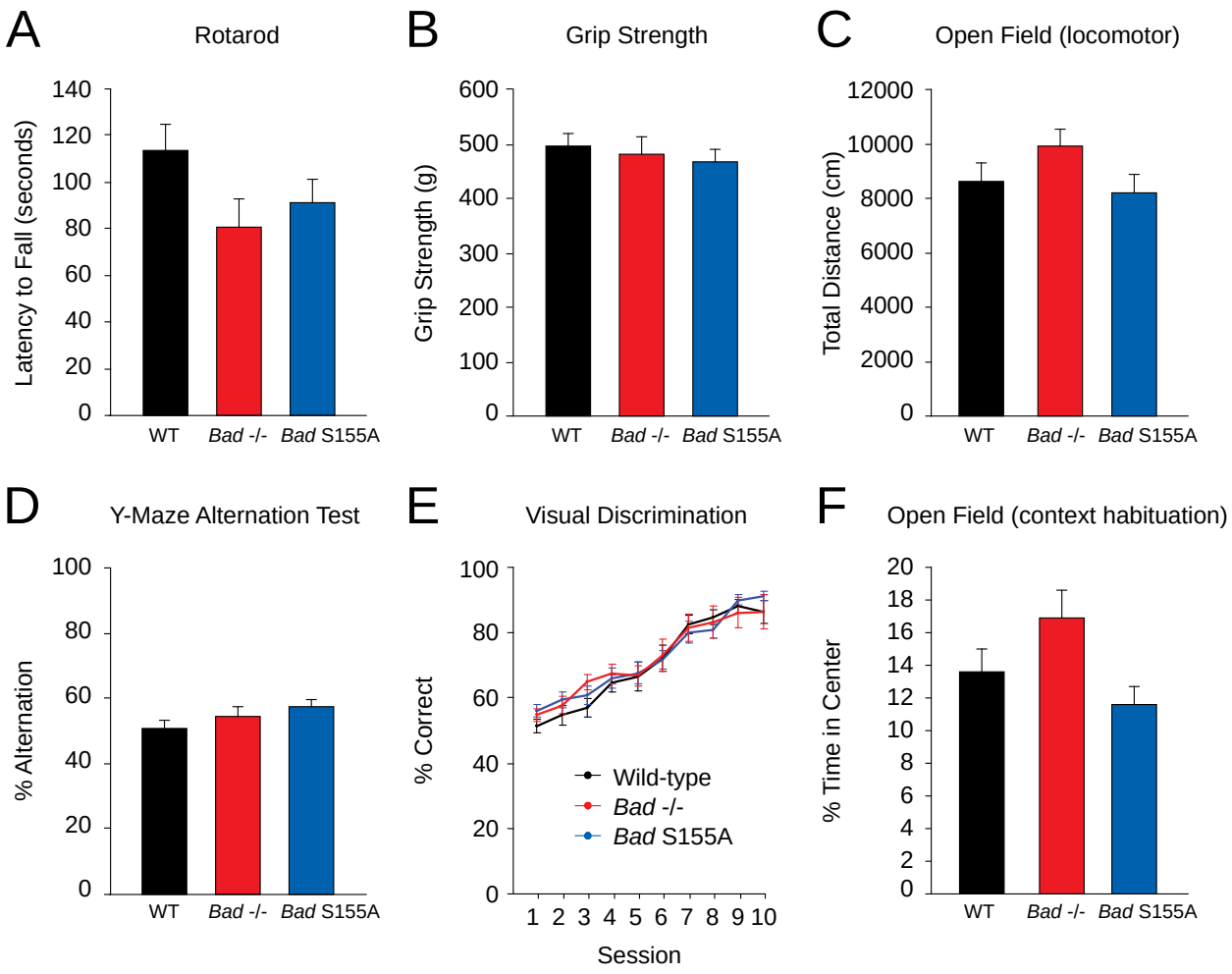

Figure S3, related to Figures 3 and 4. Unaltered Locomotor and Cognitive Functions in *Bad* Genetic Models. Wild-type, *Bad* $^{-/-}$ and *Bad* ^{S155A} mice were subjected to behavioral tests to assess motor (A-C), cognitive (D-E), and emotional (F) phenotype. (A) Latency to fall during a rotarod test as a measure of sensorimotor coordination and resistance to fatigue**.** (B) Grip strength as a measure of muscle strength**.** (C) Distance travelled in an open field chamber within 1 hr period used as a measure of context habituation and general activity**.** (D) Percent alternation of arm entries in a Y-Maze arena used as a measure of spatial, working memory**.** (E) Visual discrimination test as an index of associative learning capability. The percentage of correct responses during daily sessions of 80 trials is shown. (F) Percent time spent in the center of an open field chamber as a measure of anxiety**.** Data in A through F are presented as mean ± SEM, n=10 mice per genotype. The *p* values across genotypes in A through F are non-significant, as determined by one-way ANOVA test (A, B, D, and F) or two-way repeated measures ANOVA test (C and E).

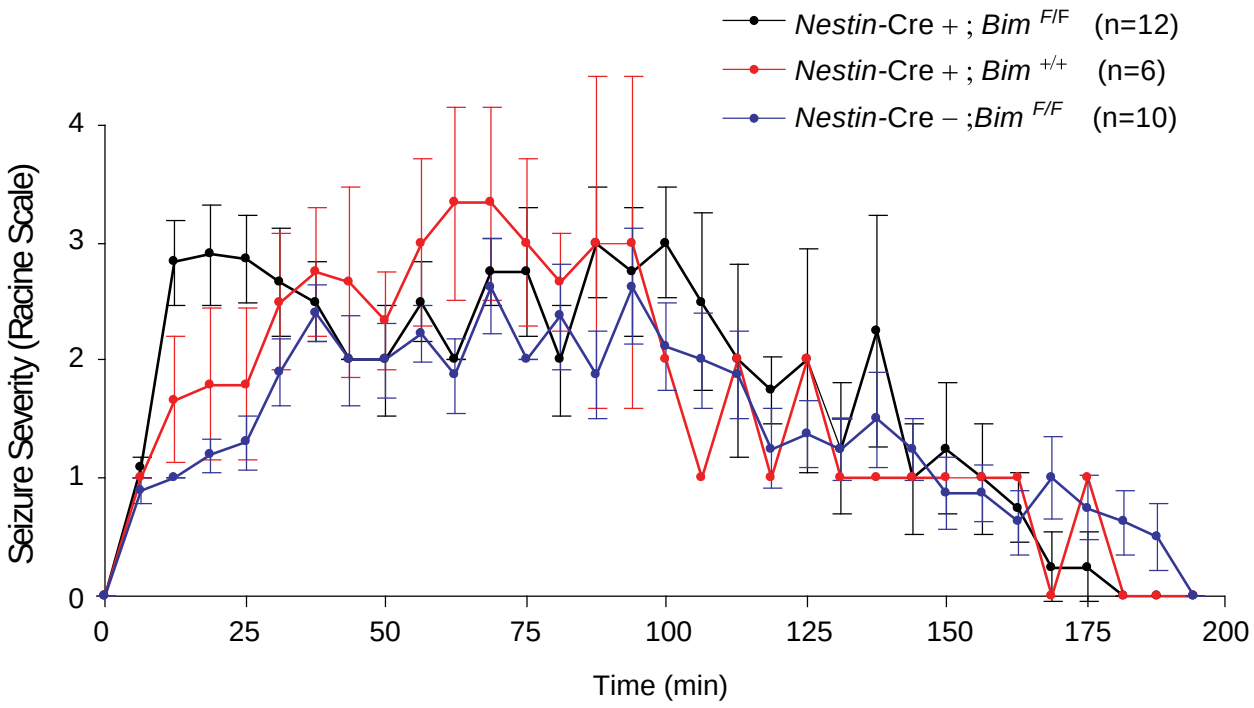

Figure S4, related to Figure 3. Sensitivity of *Bim* $^{-/-}$ Mice to Kainic Acid-Induced Acute Seizures. Behavioral seizures in mice after conditional deletion of *Bim* in the brain (*Nestin*-Cre ; *Bim* $^{F/F}$). Seizure scores were monitored as in Figure 3. Wild-type mice expressing *Nestin*-Cre alone (*Nestin*-Cre ; *Bim* $^{+/+}$) serve as controls for the effect of Cre expression.

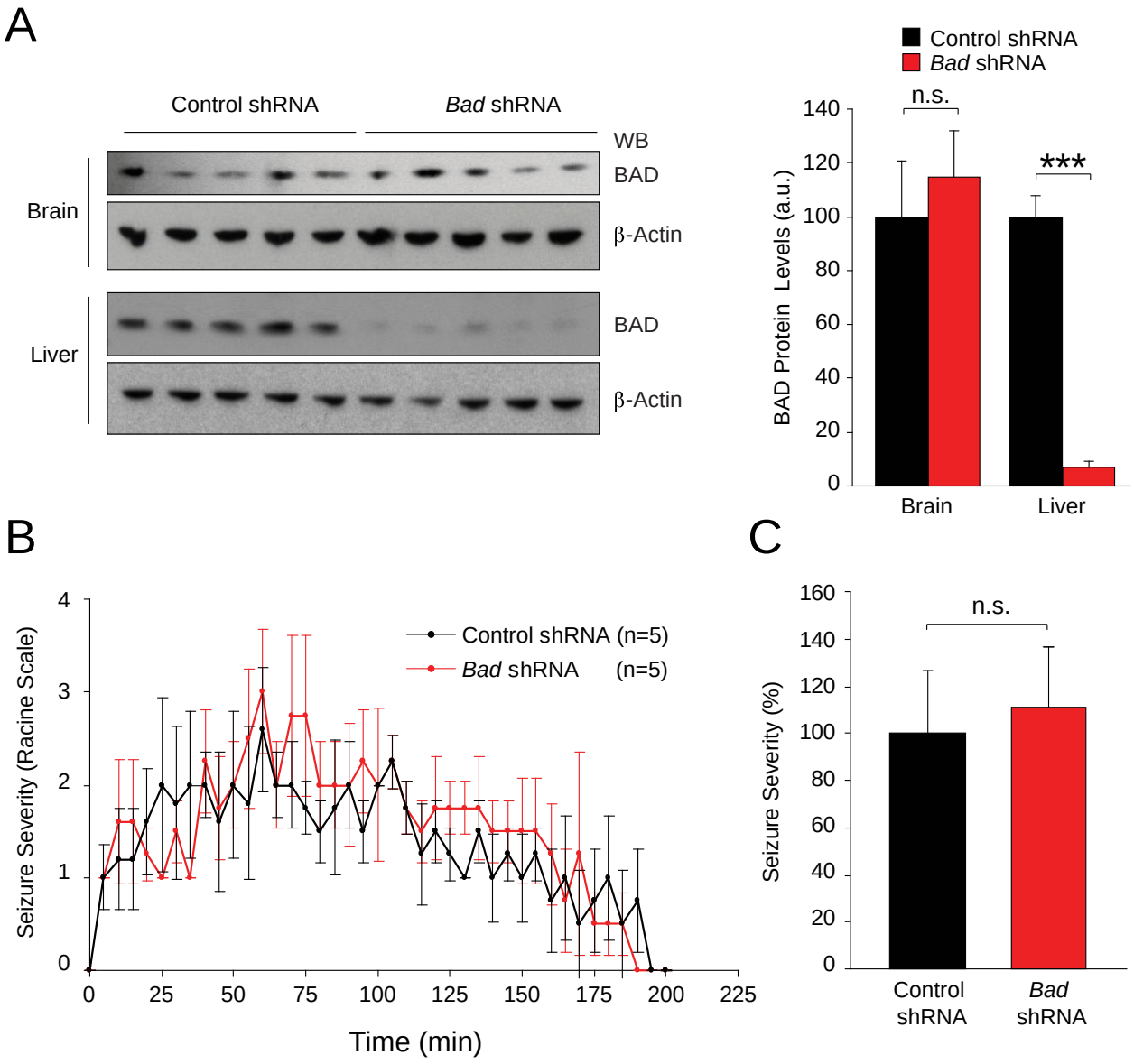

Figure S5, related to Figure 3. Seizure Resistance in the Absence of BAD is Independent of Alterations in Liver Metabolism. (A) BAD protein levels in the brain and liver isolated from mice after adenoviral delivery of *Bad* shRNA or scrambled control to the liver. (B and C) KA-induced seizure severity (B) and raw seizure scores (C) in mice treated with adenoviruses as in A. Monitoring and analysis of seizure responses were carried out as in Figure 3. Data are presented as mean ± SEM. *** $p < 0.005$; n.s., non-significant; two-tailed Student's *t*-test.

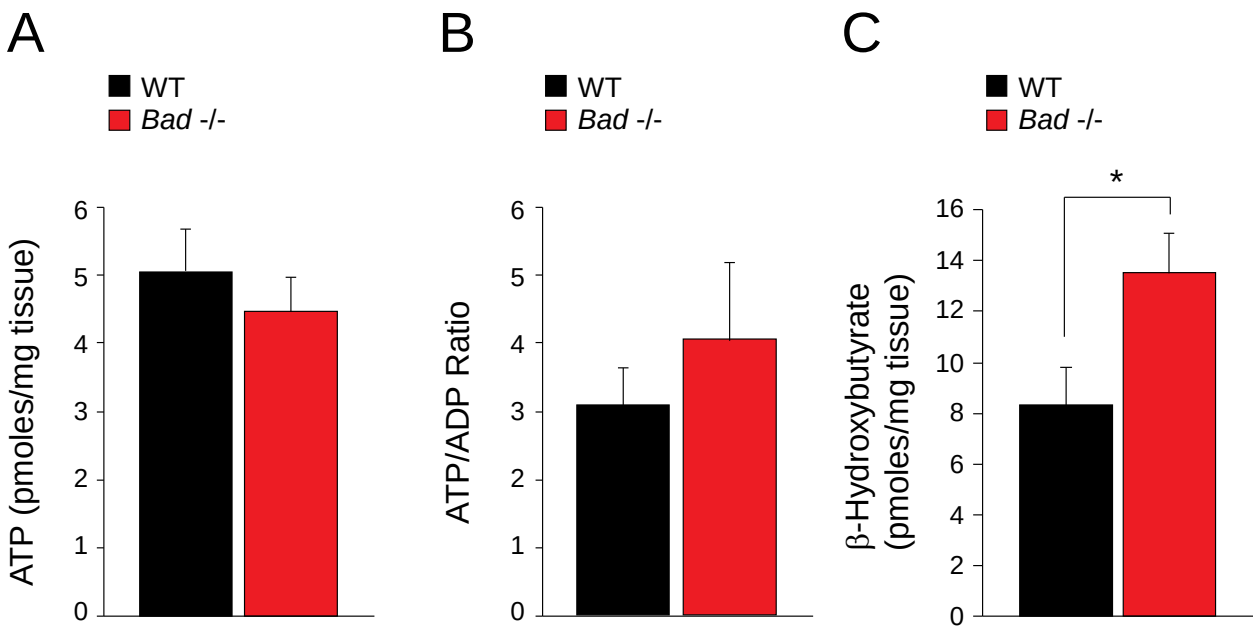

Figure S6, related to Figures 5 and 6. ATP Levels, ATP/ADP Ratio and β-Hydroxybutyrate Content in Whole Brain. ATP levels (A), ATP/ADP ratio (B) and β-hydroxybutyrate levels (C) in whole brain tissue derived from WT and *Bad* $^{-/-}$ mice. Data are presented as mean ± SEM, n=10 mice per genotype. * $p < 0.05$, two-tailed Student's *t*-test

SUPPLEMENTAL EXPERIMENTAL PROCEDURES

Western Blotting. Primary cortical neurons and astrocytes were washed once in phosphate-buffered saline (PBS) and homogenized at 4°C in a buffer containing (in mM): 20 HEPES, pH 7.4; 100 NaCl, 100 NaF, 1% Triton X-100, 1 Na_3VO_4, 5 EDTA and the Complete^{TM} protease inhibitor mixture (Roche Applied Science). The soluble fraction was mixed with SDS-containing loading buffer and proteins were resolved and western blots developed as previously described (Danial et al., 2008). The membranes were probed with the following antibodies: Pan BAD (Cell Signaling #9292), βIII-Tubulin/Tuj1 (Sigma #T2200), glial fibrillary acidic protein (GFAP) (Sigma #G3893) and β-actin (Sigma #A5441).

Liver-Specific Knock-Down of *Bad* Using shRNA. Mice were injected with adenoviruses carrying *Bad* shRNA or scrambled control at a dose of $3x10^8$ pfu/g of body weight via tail vein, an established method for acute liver-specific gene manipuation (Matsumoto et al., 2006). Five days after viral delivery, mice were treated with kainic acid and behavioral seizures were monitored as above. Parallel cohorts were also studied for metabolic consequences of acute BAD loss in the liver *in vivo* as well as hepatocyte *in vitro*, and liver-specific changes in mitochondrial carbon substrate utilization were confirmed (data not shown). BAD protein expression levels were also examined in the brain and liver 5 days after viral delivery to confirm liver-specific loss of BAD.

Behavioral Studies. Wild-type (WT), *Bad* $^{-/-}$ and *Bad* ^{S155A} mice were subjected to a comprehensive battery of behavioral tests at the Neurobehavior Laboratory of the Harvard Neurodiscovery Center. Experiments were performed on 8-10 wk old male mice (n=10 per genotype). Figure S2 depicts representative tests related to motor (A-C), cognitive (D-E), and emotional (F) phenotype.

Rotarod Test. To assess sensorimotor coordination and resistance to fatigue, the rotarod test was performed as previously described (Kornecook et al., 2010). Briefly, the latency to fall from a rod was recorded using a rotarod apparatus (Ugo Basile series; Stoelting Co. Wood Dale, IL). Mice were first exposed to the apparatus for a 5-min training trial at a constant speed of 4 rpm followed by 2 identical test trials during which the rod revolved with a steady rate of acceleration from 4 to 40 rpm over a 5-min period. The 2 test trials were separated by a 60-min interval.

***Grip Strength*.** The grip strength test was used to obtain a measure of muscle strength as previously described (Kornecook et al., 2010). Grip strength was examined using a grip meter apparatus consisting of a force transducer with a triangular wire grip (Ugo Basile series; Stoelting Co. Wood Dale, IL). Briefly, mice were lowered towards the grip bar so that the forepaws gripped the triangular handle. Mice were then pulled away by the tail horizontally until they released the handle and the strength of their grip in grams was measured. Five scores were recorded per animal in consecutive sequence.

***Open Field Activity Test*.** To assess overall locomotor activity, anxiety, and context habituation, an open field test was used to study mice confined to a novel arena using a standard mouse open field chamber (Med Associates Inc, Georgia, VT) (Kornecook et al., 2010). Briefly, a single 1-h session was initiated by placing a mouse in the center of the arena. The animal was allowed free exploration in the environment and a computer-assisted infra-red tracking system was used to record the number of beam breaks (activity) in user defined zones (center, periphery) as well as the number of hindlimb rearings. The distance covered in the open field chamber was used as an index of locomotor function (panel C) and the percent time spent in the center of the open field chamber was used as an indication of context habituation and anxiety (panel F), as mice tend to stay near walls rather than in the center of an open field.

Y-Maze Spontaneous Alternation Test. To assess spatial working memory, a Y-maze test was performed as previously described (Kornecook et al., 2010). This test is based on the spontaneous tendency of rodents to alternate arm entries in a Y-maze arena. Briefly, mice were allowed to explore a plexiglas Y-shaped maze consisting of 3 equidistant arms for 6 min in a single session. The distance travelled and the sequence of arm entries during testing were automatically recorded by the CleverSys computer-assisted videotracking system (CleverSys, Inc.Reston, VA). The percentage of alternations was used as an index of working memory performance.

***Visual Discrimination Test*.** To examine learning capabilities, a visual discrimination test was performed as previously described (Dillon et al., 2009). Briefly, mice were required to discriminate between reinforced and non-reinforced levers to obtain food reward. Prior to training, food-restricted mice were exposed to the operant chamber for 45 min without access to the operant levers. During this habituation session, mice received 24 exposures to a 1-s

receptacle-light stimulus with an inter-trial interval (ITI) of 120 s. The presentation of the receptacle-light stimulus coincided with the delivery of a 20-mg food pellet. Following habituation, mice received two, daily shaping sessions during which only one lever (left or right) was presented at a time concurrently with random light presentation. During shaping sessions a single lever was available indefinitely until the subject made a response. Following each response the lever was retracted, food receptacle light turned on, and a single 20-mg food pellet was delivered. Each additional trial began 10 s following the retrieval of the food reward. The random presentation of a stimulus light for only half of the shaping trials prevented the animals from elaborating discrimination strategies prior to the beginning of training. Throughout this continuous reinforcement procedure each lever-press was followed by the delivery of a food pellet in the receptacle. Shaping sessions lasted for a maximum of 30 min or 60 trials.

***Statistical Analysis of Neurobehavioral Tests*.** In all cases, mean ± SEM are presented (n=10 mice per genotype). For rotarod, grip strength and Y-maze alternation tests, one-way analysis of variance (ANOVA) statistical test was performed. For open field and visual discrimination tests, two-way repeated measures ANOVA (one factor repetition) test was carried out.

ATP Measurements and Determination of ATP/ADP Ratio. ATP levels and ATP/ADP ratio in whole brain were determined as previously described (Schultz et al., 1993). Briefly, the whole brain tissue was deproteinizated in 0.9 N $HClO_4$ followed by neutralization with 2N KOH-0.5 M triethanolamine, and the aqueous phase was assayed using a luminescence-based assay for ATP measurements (Cell Titer Glo, Promega, Madison, WI). The values were then normalized by tissue weight. For ADP measurements, a pyruvate kinase-driven reaction was used with phosphoenolpyruvate as substrate to first convert the ADP in the samples to ATP, and the samples were assayed for ATP as described above. The difference between ATP values before and after pyruvate kinase reaction was used to deduce the ADP content in the original sample.

Determination of β-Hydroxybutyrate Levels. β-Hydroxybutyrate levels in $HClO_4$-deproteinized whole brain tissue samples were determined using a colorimetric assay-based kit per manufacturer's instructions (Wako Diagnostics, Richmond, VA). Briefly, 10 μl of sample was mixed with 135 μl of reagent R1 provided in the kit and incubated at 37°C for 5 min. Then 45 μl of reagent R2 was added to the mixture followed by 2 min incubation at 37°C. The optical density of the reaction was then determined at 405 nm every 20 seconds for 3 min and the slope

of the reaction in the linear range was used to calculate β-hydroxybutyrate concentrations using standards of known concentrations as a reference. The total levels of β-hydroxybutyrate were normalized to the tissue sample weight.

SUPPLEMENTAL REFERENCES

Danial, N.N., Walensky, L.D., Zhang, C.Y., Choi, C.S., Fisher, J.K., Molina, A.J., Datta, S.R., Pitter, K.L., Bird, G.H., Wikstrom, J.D., *et al.* (2008). Dual role of proapoptotic BAD in insulin secretion and beta cell survival. Nat. Med. *14*, 144-153.

Dillon, G.M., Shelton, D., McKinney, A.P., Caniga, M., Marcus, J.N., Ferguson, M.T., Kornecook, T.J., and Dodart, J.C. (2009). Prefrontal cortex lesions and scopolamine impair attention performance of C57BL/6 mice in a novel 2-choice visual discrimination task. Behav. Brain Res. *204*, 67-76.

Kornecook, T.J., McKinney, A.P., Ferguson, M.T., and Dodart, J.C. (2010). Isoform-specific effects of apolipoprotein E on cognitive performance in targeted-replacement mice overexpressing human APP. Genes Brain Behav. *9*, 182-192.

Matsumoto, M., Han, S., Kitamura, T., and Accili, D. (2006). Dual role of transcription factor FoxO1 in controlling hepatic insulin sensitivity and lipid metabolism. J. Clin. Invest. *116*, 2464-2472.

Schultz, V., Sussman, I., Bokvist, K., and Tornheim, K. (1993). Bioluminometric assay of ADP and ATP at high ATP/ADP ratios: assay of ADP after enzymatic removal of ATP. Analyt. Biochem. *215*, 302-304.